

## TABLE OF CONTENTS

CERTIFICATION.....	i
ABSTRACT.....	iii
ACKNOWLEDGEMENT.....	iv
CHAPTER 1 .....	6
INTRODUCTION .....	6
1.1    Background of study .....	6
1.2    Problem statement .....	6
1.2.1    Problem Identification.....	6
1.2.2    Significance of the Project .....	7
1.3    Objectives and scope of study .....	7
1.4    Relevancy of project.....	8
1.5    Feasibility of the Project.....	8
CHAPTER 2 .....	10
LITERATURE REVIEW AND THEORY.....	10
2.1    Literature review on past work in study .....	10
2.2    Relevancy of the literature.....	15
2.3    Computational fluid dynamics (CFD).....	16
2.4    FLUENT and GAMBIT Software.....	16
2.5    Advantages numerical method (CFD).....	17
2.6    Bluff Body: Viscous Flow Characteristics (Immersed Bodies) .....	18
2.7    Lift force.....	19
2.8    Drag force.....	20
CHAPTER 3 .....	21
METHODOLOGY.....	21

3.1	Procedure identification .....	21
3.2	Key milestone .....	21
3.3	The project flow .....	22
3.4	Project Activities .....	22
3.4.1	Modeling Using GAMBIT.....	22
3.4.2	Specifying the problem and run the model using FLUENT .....	23
3.4.3	Construct the graph of relationship between parameters.....	24
3.4.4	Discussion.....	24
3.5	Gantt Chart .....	25
3.6	Tools and Equipment Needed .....	25
CHAPTER 4 .....		26
RESULTS AND DISCUSSION .....		26
4.1	Properties of Fluid and Square Cylinder .....	26
4.2	Cutting and Rotation Angle for Square Cylinder .....	27
4.2.1	Analysis Using GAMBIT .....	28
4.2.2	Analysis Using FLUENT .....	28
4.3	Simulation Model.....	29
4.4	0 <sup>0</sup> Cutting Model.....	29
4.4.1	0 <sup>0</sup> Rotation Model .....	29
4.4.2	15 <sup>0</sup> Clockwise Rotation Model.....	31
4.4.3	285 <sup>0</sup> Clockwise Rotation Model.....	33
4.5	0 <sup>0</sup> Cutting Model.....	35
4.5.1	0 <sup>0</sup> Rotation Model .....	35
4.5.2	15 <sup>0</sup> Clockwise Rotation Model.....	37
4.5.3	285 <sup>0</sup> Clockwise Rotation Model.....	39
4.6	45 <sup>0</sup> Cutting Model.....	41
4.6.1	0 <sup>0</sup> Rotation Model .....	41

4.6.2	15 <sup>0</sup> Clockwise Rotation Model.....	43
4.6.3	285 <sup>0</sup> Clockwise Rotation Model.....	45
4.7	Discussion .....	47
CHAPTER 5 .....		52
CONCLUSION AND RECOMMENDATION.....		52
5.1	Conclusion.....	52
5.2	RECOMMENDATION.....	52
REFERENCES.....		53
APPENDICES.....		54

## LIST OF FIGURE

Figure 1: Flow in A Channel With Built-In Square Obstacle.....	12
Figure 2: Flow Configuration (Left) And Close-Up Of Grid Near Cylinder (Right)	14
Figure 3: Axis of the Free Stream Approach Velocity U.....	18
Figure 4: Project Flow.....	22
Figure 5: Laminar flow .....	24
Figure 6: Fluid Flow for Square Cylinder.....	27
Figure 7: Different Cutting Angles which are, $0^{\circ}$ , $30^{\circ}$ and $45^{\circ}$ .....	27
Figure 8: Contour of total pressure of $0^{\circ}$ cutting and $0^{\circ}$ rotation.....	30
Figure 9: Contour of total pressure of $0^{\circ}$ cutting and $0^{\circ}$ rotation square block.....	30
Figure 10: Contour of total pressure of $15^{\circ}$ clockwise rotation .....	31
Figure 11: Contour of total pressure of $15^{\circ}$ clockwise rotation square block.....	32
Figure 12: Contour of total pressure of $285^{\circ}$ clockwise rotation .....	33
Figure 13: Contour of total pressure of $125^{\circ}$ clockwise rotation square block.....	34
Figure 14: Contour of total pressure of $30^{\circ}$ cutting and $0^{\circ}$ rotation.....	35
Figure 15: Contour of total pressure of $30^{\circ}$ cutting and $0^{\circ}$ rotation square block.....	36
Figure 16: Contour of total pressure of $15^{\circ}$ clockwise rotation .....	37
Figure 17: Contour of total pressure of $15^{\circ}$ clockwise rotation square block.....	38
Figure 18: Contour of total pressure of $285^{\circ}$ clockwise rotation .....	39
Figure 19: Contour of total pressure of $285^{\circ}$ clockwise rotation square block.....	40
Figure 20: Contour of total pressure of $0^{\circ}$ rotation .....	41
Figure 21: Contour of total pressure of $45^{\circ}$ cutting and $0^{\circ}$ rotation square block.....	42
Figure 22: Contour of total pressure of $15^{\circ}$ clockwise rotation .....	43
Figure 23: Contour of total pressure of $15^{\circ}$ clockwise rotation square block.....	44
Figure 24: Contour of total pressure of $285^{\circ}$ clockwise rotation .....	45
Figure 25: Contour of total pressure of $285^{\circ}$ clockwise rotation square block.....	46
Figure 26: Pressure in x and y-direction .....	47
Figure 27: Rotation vs Drag Coefficient.....	50
Figure 28: Rotation vs Lift Coefficient.....	51

## LIST OF TABLE

Table 1: Data properties of fluid which is air .....	26
Table 2: List of lift and drag force and coefficient .....	48

# CHAPTER 1

## INTRODUCTION

### 1.1 Background of study

Flow around a square cylinder has been subjected to extensive research efforts in a wide range of engineering disciplines. Different studies show that this flow configuration has many engineering applications such as building structure and still presents one of the major challenges in fluid mechanics.

A square cylinder is a basic example of such flows, its industrial applicability ranging from wind induced motion to turbulent sound generation [1]. Fluid flow past a square cylinder has been the subject of fundamental research because of the intricate mechanisms in the wake that result in a variety of unexpected phenomena. Examples are wake unsteadiness even at Reynolds numbers, detachment of the free shear layer and the consequent shedding of vortices, generation of harmonics, three-dimensionality in 2D geometries, onset of chaos, and the approach to turbulence [2].

### 1.2 Problem statement

#### 1.2.1 Problem Identification

All objects towards the fluid flow experience forces due to the interaction between the objects and the flow. The forces can be generally categorized as drag and lift forces. Reduction of the existing forces acting on an object can be done by controlling the boundary layer developing on the object surface. Object shape modification will control the boundary layer development on the object surface [3].

A lot of tall buildings are square in horizontal cross sectional shapes. Due to dominant, wind around their area; they will experience dominant wind buildings in

certain directions. Wind loading causes moment and need to be considered in design of building structure. Aerodynamic forces on the object can be reduced to a particular cutting and rotation hence it will benefit for a technical consideration.

### 1.2.2 Significance of the Project

Study the flow characteristics of the square cylinder such as tall building structure when the structure is being cut and rotate need to be done. Furthermore, numerical study for different cutting and rotation angle not has been study yet.

The significance of this project that in the future it could help the engineers and designers in designing the structure building that will benefit for technical and economic consideration. The flow situation is owing to its related technical problems associated with energy conservation and structural design.

## 1.3 Objectives and scope of study

- 1.3.1
- a) To study on the flow characteristics of a bluff body from a square cylinder using numerical method.
  - b) To compare and study flow characteristics for each cutting and rotating angle of the bluff body of the cylinder using numerical method since it will reduce time and cost. Characteristics of the flow will be study by the simulation. CFD simulation will show the details about total pressure profiles.
- 1.3.2
- a) Modeling of the bluff body for square cylinder with various cutting and rotation using GAMBIT.
  - b) Simulation and analysis of the chosen models under various airflow using FLUENT.
  - c) Analysis and comparison results of simulation. Characteristics from the simulation are drag and lift force. Scope of study includes studying the contour of total pressure.
  - d) Data from FLUENT will be taken to calculate drag and lift coefficient.

## **1.4 Relevancy of project**

This project is relevant to the study of fundamental and application of Fluid Mechanics as well as the study on the flow characteristic of a bluff body cut from a square cylinder.

Motion of bluff, non-aerodynamic objects through fluids is encountered very extensively in engineering practice. Submarines, ships, passenger aircraft, automobiles and missiles are examples where the object is in motion through a stationary fluid medium. High-rise buildings, chimneys and tube banks in heat exchangers are examples where the fluid is in motion [5].

Besides, there also had many research on this topic before and basically there will be some variations on the result as the method and approach being used are different. Traditionally, both experimental and analytical methods have been used to study the various aspects of fluid flow over bluff body cut. With the advent of digital computers, the computational (numerical) aspects have emerged as another viable approach. With hope that by using GAMBIT and FLUENT, the result obtained would be accurate.

## **1.5 Feasibility of the Project**

The project is feasible as it utilizes from the simulation by using numerical technique called computational fluid dynamics, CFD which is GAMBIT and FLUENT software. The simulation will show the flow characteristics for the bluff body cut. The project is feasible within the time frame given (1 year) which divided into 2 sections;

- 1) Deep research/study of the project.
- 2) The analysis for the detail characteristics which are for the bluff body cut on the square cylinder.



The project is low in cost since it is using simulation and analysis for overall project. This project is beneficial to the industry as the flow across bluff body cut for square cylinder effect the engineering design. For example flow across tall building structure.

## CHAPTER 2

### LITERATURE REVIEW AND THEORY

#### 2.1 Literature review on past work in study

Most of the studies published in literature have dealt with the issue of the force that occurred at the flow of the circular cylinders and spheres. There are very few studies for the flow of the square block or cylinder. Previous study by A Pudjanarsa shows the experimental study on the effect of turning angle on drag and lift forces for various cut angles on spheres. An experimental study on the effect of turning angle on drag and lift forces for various cut angles on spheres is performed. Five different cut angles on different spheres were applied including: 30°, 45°, 53°, 55°, and 75°. Drag and lift forces were measured using a wind tunnel force balance and the wind speed was set so that a corresponding Reynolds number of  $5.3 \times 10^4$  was achieved. Wind turning angle was varied from 0° to 60°. Experimental results show that, in general, drag and lift forces increase as the turning angle increases. At 0° turning angle,  $C_d$  minimum is attained at a cut angle of 53° and is ~32 per cent less than  $C_d$  without cut angle. The maximum  $C_l$  is attained at a cut angle of 75° for a turning angle of 50° for approximately 0.68. This value of  $C_{l,max}$  is about 855 per cent higher than that of the same turning angle for a cut angle of 30°. At a particular turning angle, lift attains a maximum and beyond that turning angle-drag and lift forces decrease. Minimum value of drag and lift forces reached at the cut angle of 30° for all turning angles [1].

S. Aiba and H. Watanabe are also carried out experimental study on flow characteristics of a bluff body cut from a circular cylinder. This is a report on an investigation of the flow characteristics of a bluff body cut from a circular cylinder. They study the flow characteristics which are base pressure coefficient and the drag coefficient around a two-dimensional bluff body with the cross section which is relatively easy to manufacture. The volume removed from the cylinder is equal to  $d/2(1 - \cos \Theta_s)$ , where  $d$  and  $\Theta_s$ , are the diameter and the angular position (in the

case of a circular cylinder,  $\Theta_s = 0$  deg), respectively.  $\Theta_s$  ranged from 0 deg to 72.5 deg and  $Re$  (based on  $d$  and the upstream uniform flow velocity  $U_\infty$ ) from  $2.0 \times 10^4$  to  $3.5 \times 10^4$ . It is found that a singular flow around the cylinder occurs at around  $\Theta_s = 53$  deg when  $Re > 2.5 \times 10^4$ , and the base pressure coefficient ( $-C_{pb}$ ) and the drag coefficient  $C_D$  take small values compared with those for other  $\Theta_s$ . In the vicinity of  $\Theta_s = 53$  deg, the value of  $C_D$  for each model is minimum and about 50 percent of that for the circular cylinder. The critical Reynolds number  $Re_{cc}$  is around  $Re = 2.5 \times 10^4$  in the case of  $\Theta_s = 53$  deg [6].

The paper by Jyoti Chakraborty, Nishith Verma and R. P. Chhabra also studied about the flow for the circular cylinder. This paper shows the numerical study of wall effects in flow past a circular cylinder in a plane channel. It describes about the numerical study on the steady flow of an incompressible Newtonian fluid past a circular cylinder confined in a plane rectangular channel. Using FLUENT (version 6), two-dimensional steady state computations were carried out for an uniform inlet velocity and for different values of the Reynolds numbers in the range between 0.1 and 200 and blockage ratios (ratio of the channel width to the cylinder diameter) in the range between 1.54 and 20. The flow parameters such as drag coefficient, length of the recirculation zone, and the angle of separation are presented as functions of the Reynolds number and blockage ratio. The total drag coefficient ( $C_D$ ) was found to decrease with an increase in the blockage ratio ( $\lambda$ ) for a fixed value of the Reynolds number ( $Re$ ) and to decrease with increasing Reynolds number for a fixed value of  $\lambda$ . Similarly, for a fixed value of  $\lambda$ , both the angle of separation and the length of the recirculation zone increase with the increasing Reynolds number [7].

Shuyang Cao and Yukio Tamura also studied about the flow for the circular cylinder. The paper is about the flow around a circular cylinder in linear shear flows at subcritical Reynolds number. Vortex shedding and aerodynamic forces around a circular cylinder in linear shear flows with its axis normal to the plane of the velocity shear profile are investigated numerically and experimentally at subcritical Reynolds number. Large eddy simulation using a dynamic Smagorinsky subgrid model is performed to supply physical explanations of the flow phenomena. The shear parameter  $\beta$ , which is based on the velocity gradient, cylinder diameter and upstream

mean velocity at the center plane of the cylinder, varies from 0 to 0.27. It is found that the Strouhal number shows no significant variation with shear parameter. The stagnation point shifts to the high-velocity side and it greatly influences the aerodynamic force acting on the cylinder. There is a lift force due to the asymmetrical distribution of pressure around the cylinder, and it acts from the high-velocity side to the low-velocity side at subcritical Reynolds number [8].

Although there are many papers about the circular cylinder and spherical, there are some of the papers study about the flow for square cylinder. A. K. Saha, K. Muralidhar, and G. Biswas, had been study about the flow past a square cylinder. One of the paper work discuss about vortex structures and kinetic energy budget in two-dimensional flow past a square cylinder. Direct Numerical Simulation of unsteady, two-dimensional flow past a square cylinder placed centrally in a channel has been carried out using a higher order finite difference scheme. A Reynolds number of 100 have been considered in the computation. The flow in the wake is found to be unsteady with a strong periodic component. The instantaneous vorticity field at this Reynolds number is seen to be spatially coherent. Hence, the primary conclusion of the present study is that the unsteady flows with one or a few dominating frequencies (periodic or quasi-periodic) are statistically similar to a fully turbulent flow. To assess the similarity further, the energy transfer mechanism between the mean motion and the fluctuations has been studied through different terms associated with kinetic energy budget of the fluctuating velocities. The total pressure, the advection of the time-mean flow and production terms are found to be primarily responsible for the energy cascade. In contrast, diffusion and dissipation do not appear to have a significant in influence on the energy transfer mechanism [5].

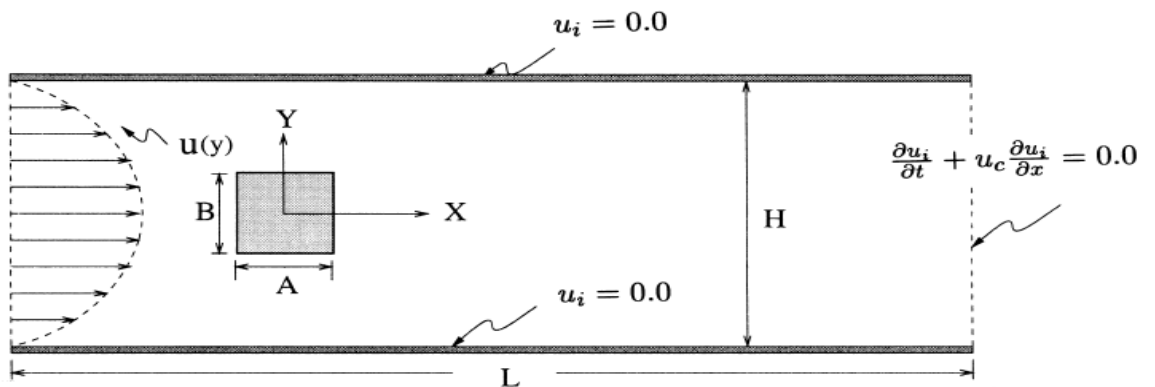


Figure 1: Flow in A Channel With Built-In Square Obstacle

A.K. Saha, K. Muralidhar, and G. Biswas also studied about the transition and chaos in two-dimensional flow past a square cylinder. The unsteady wake of a long square cylinder has been numerically analyzed in the present study. Velocity signals at selected locations in the near-wake and the instantaneous forces on the cylinder have been recorded from the numerical model at various Reynolds numbers. These form the basis of investigating the dynamic behavior of the flow system. Results of the present work show the following. Flow past a square cylinder undergoes a sequence of transitions from a steady pattern up to a Reynolds number of 40 to a chaotic one around a Reynolds number of 600. The transition to chaos is manifested through a quasi-periodic route that includes the frequency-locking phenomenon. The transition to chaos in the wake of a bluff object is related to the three-dimensionality of the flow. In a 2D simulation, this appears in the form of new harmonics in the velocity traces. The quasi-periodic route to chaos has been established through different characterization tools, such as the spectra, autocorrelation function, time-delay reconstruction, and the Poincaré section. Chaotic behavior is quantified through the calculation of Lyapunov exponent and fractal dimension [2].

In previous investigation made by Sumeet Thete, Kaustubh Bhat and M.R. Nandgaonkar show the 2 dimensional simulation of fluid flow over a rectangular prism. This paper is a part of an elaborate research involving simulation and practical testing of flows across solid objects. The research presented here deals with only the numerical modeling of such flows by development of code specifically for this purpose. The objective of this paper is to model the unsteady flow of incompressible fluid across a rectangular prism using simple collocated grid arrangement for Navier-Stokes equation. The flow has been modeled numerically and flow visualizations have been generated for increasing values of Reynolds number for a fluid at high kinematic viscosity. These results have been validated against previously probed values of the Strouhal number versus the Reynolds number. Also, an investigation has been made into the flow characteristics of a fluid at low kinematic viscosity in comparison with the highly viscous fluid at the same Reynolds number. The simulations have been performed at low values of Reynolds number. A prism of unit depth was chosen. The numerical

investigation provides substantial information regarding the vortex shedding characteristics with increasing values of Reynolds number [9].

A. Sohankar, C. Norberg and L. Davidson have carried out a study of blockage, onset of vortex shedding and outlet boundary condition for low Reynolds number flow around a square cylinder at incidence. Calculations of unsteady 2D flow around a square cylinder at incidence ( $\alpha = 0^\circ$ - $45^\circ$ ) are presented. The Reynolds numbers are low ( $Re = 45$ - $200$ ) so that the flow is presumably laminar. A von Kârmân vortex sheet is predicted behind the cylinders with a periodicity which agrees well with experiments. An incompressible simplec code is used with a non-staggered grid arrangement. A third-order quick scheme is used for the convective terms. The time discretization is implicit and a second-order Crank-Nicolson scheme is employed. At the outlet of the computational domain a convective Sommerfeld boundary condition is compared with a traditional Neumann condition. The convective boundary condition is shown to be more effective in reducing the CPU time, reducing the upstream influence of the outlet and thus reducing the necessary downstream extent of the domain. A study of the effects of spatial resolution and blockage is also provided. The onset of vortex shedding is investigated by using the Stuart-Landau equation at various angles of incidence and for a solid blockage of 5%. A number of quantities such as Strouhal number and drag, lift and moment coefficients are calculated [10].

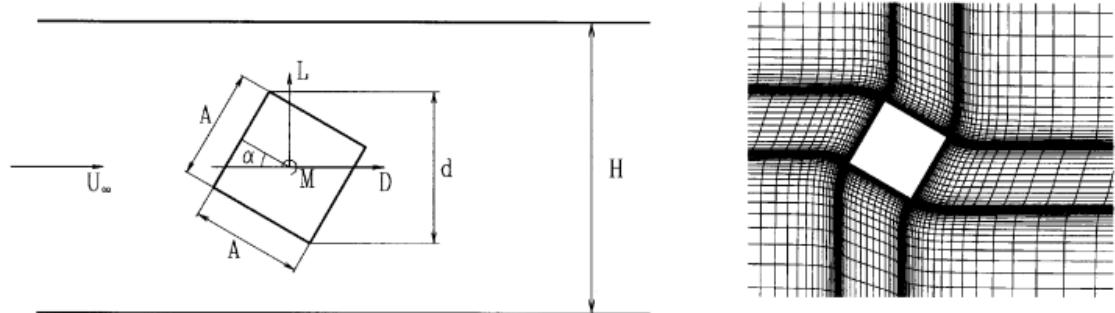


Figure 2: Flow Configuration (Left) And Close-Up Of Grid Near Cylinder (Right)

Sushanta Dutta, P. K. Panigrahi and K. Muralidhar experimentally investigated the flow past a square cylinder at an angle of incidence. Flow past a square cylinder placed at an angle to the incoming flow is experimentally investigated using particle image velocimetry, hot wire anemometry, and flow visualization. The Reynolds number based on cylinder size and the average incoming velocity is set equal to 410. Data for four cylinder orientations ( $\Theta=0^\circ, 22.5^\circ, 30^\circ$  and  $45^\circ$ ) and two aspect ratios (AR=16 and 28) are reported. Results are presented in terms of drag coefficient, Strouhal number, time averaged velocity, stream traces, turbulence intensity, power spectra, and vorticity field. In addition, flow visualization images in the near wake of the cylinder are discussed. The shape and size of the recirculation bubble downstream of the cylinder are strong functions of orientation. A minimum in drag coefficient and maximum in Strouhal number is observed at a cylinder orientation of  $22.5^\circ$ . The  $v$ -velocity profile and time-average stream traces show that the wake and the separation process are asymmetric at orientations of  $22.5^\circ$  and  $30^\circ$ . The corresponding power spectra show additional peaks related to secondary vortical structures that arise from nonlinear interaction between the Karman vortices. The flow visualization images show the streamwise separation distance between the alternating vortices to be a function of cylinder orientation. Further, the flow approaches three dimensional early which is closer to the cylinder surface for the  $22.5^\circ$  orientation. The drag coefficient decreases with an increase in aspect ratio, while the Strouhal number is seen to increase with aspect ratio. The turbulence intensity is higher for the large aspect ratio cylinder and the maximum turbulence intensity appears at an earlier streamwise location. The overall dependence of drag coefficient and Strouhal number on orientation is preserved for the two aspect ratios studied [11].

## **2.2 Relevancy of the literature**

It is observed that there are two papers of earlier work for flow characteristics for cutting and rotation angle and it only focused on spherical and circular cylinder by using experimental method. It is because most of the engineering application on the circular and spherical shape. For example are supporting column for offshore constructions, bridge piles, and tubes in heat exchangers. These literature reviews indicates the important of cylinder cutting and rotation for bluff bodies. However, for

a square cylinder, a joint study of cylinder rotation and cutting is not available. Study the flow characteristics for rotation and cutting of the square cylinder also important especially for building structures since the shape is square cylinder. The previous works for square cylinder only focused on rotation of the cylinder.

### **2.3 Computational fluid dynamics (CFD)**

Computational fluid dynamics (CFD) is one of the branches of fluid mechanics that uses numerical methods and algorithms to solve and analyze problems that involve fluid flows. Computers are used to perform the millions of calculations required to simulate the interaction of liquids and gases with surfaces defined by boundary conditions. Even with high-speed supercomputers only approximate solutions can be achieved in many cases. Ongoing research, however, may yield software that improves the accuracy and speed of complex simulation scenarios such as transonic or turbulent flows. Initial validation of such software is often performed using a wind tunnel with the final validation coming in flight test.

The fundamental basis of almost all CFD problems is the Navier-Stokes equations, which define any single-phase fluid flow. These equations can be simplified by removing terms describing viscosity to yield the Euler equations. Further simplification, by removing terms describing vorticity yields the full potential equations. Finally, these equations can be linearized to yield the linearized potential equations.

### **2.4 FLUENT and GAMBIT Software**

FLUENT is a computational fluid dynamics (CFD) software package to simulate fluid flow problems. It uses the finite-volume method to solve the governing equations for a fluid. It provides the capability to use different physical models such as incompressible or compressible, inviscid or viscous, laminar or turbulent, etc. Geometry and grid generation is done using GAMBIT which is the preprocessor bundled with FLUENT [12].



There are seven steps for modeling using GAMBIT and FLUENT:

1. Create Geometry in GAMBIT
2. Mesh Geometry in GAMBIT
3. Set Boundary Types in GAMBIT
4. Set Up Problem in FLUENT
5. Solve
6. Analyze Results
7. Refine Mesh

## **2.5 Advantages numerical method (CFD)**

FLUENT uses unstructured, hybrid modeling technology, models can be built that conform to arbitrary geometric shapes and other complex surfaces. As a result, the CFD model will have accuracy it needs, where it is needed. CFD also very compelling, non-intrusive, virtual modeling technique with powerful visualization capabilities and engineers can evaluate the performance of a wide range of HVAC/IAQ system configurations on the computer without the time, expense, and disruption required to make actual changes onsite. The many reasons CFD is being widely used today are as follows:

1. CFD predicts performance before modifying or installing systems:
  - Without modifying and/or installing actual systems or a prototype, CFD can predict which design changes are most crucial to enhance performance.
2. CFD provides exact and detailed information about HVAC design parameters:
  - The advances in HVAC/IAQ technology require broader and more detailed information about the flow within an occupied zone, and CFD meets this goal better than any other method, (i.e., theoretical or experimental methods).

CFD also saves cost and time. CFD costs much less than experiments because physical modifications are not necessary.

## 2.6 Bluff Body: Viscous Flow Characteristics (Immersed Bodies)

In general, a body immersed in a flow will experience both externally applied forces and moments as a result of the flow about its external surfaces. The typical terminology and designation of these forces and moments are given in the figure 3.

The orientation of the axis for the drag force is typically along the principal body axis, although in certain applications, this axis is aligned with the principal axis of the free stream approach velocity  $U$ .

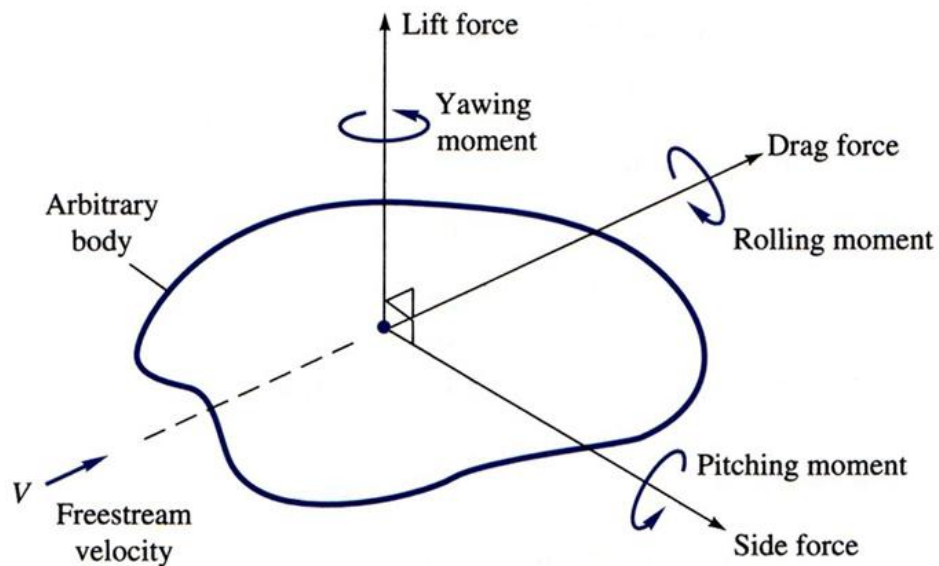


Figure 3: Axis of the Free Stream Approach Velocity  $U$

Since in many cases the drag force is aligned with the principal axis of the body shape and not necessarily aligned with the approaching wind vector. Review all data carefully to determine which coordinate system is being used: body axis coordinate system or a wind axis coordinate system.

These externally applied forces and moments are generally a function of

- a. Body geometry
- b. Body orientation
- c. Flow conditions

These forces and moments are also generally expressed in the form of a non-dimensional force/moment coefficient, e.g. the drag and lift coefficient.

## 2.7 Lift force

Lift depends on the density of the air, the square of the velocity, the air's viscosity and compressibility, the surface area over which the air flows, the shape of the body, and the body's inclination to the flow. In general, the dependence on body shape, inclination, air viscosity, and compressibility is very complex.

One way to deal with complex dependencies is to characterize the dependence by a single variable. For lift, this variable is called the lift coefficient, designated "Cl." This allows us to collect all the effects, simple and complex, into a single equation. The lift equation states that lift L is equal to the lift coefficient Cl times the density times half of the velocity V squared times the area A.

$$L = C_L \times \rho \times \frac{V^2}{2} \times A$$

For given air conditions, shape, and inclination of the object, we have to determine a value for Cl to determine the lift. For some simple flow conditions and geometries and low inclinations, aerodynamicists can determine the value of Cl mathematically. But, in general, this parameter is determined experimentally.

The lift coefficient is a number that aerodynamicists use to model all of the complex dependencies of shape, inclination, and some flow conditions on lift. This equation is simply a rearrangement of the lift equation where we solve for the lift coefficient in terms of the other variables. The lift coefficient Cl is equal to the lift L divided by the quantity: density times half the velocity V squared times the area A.

$$C_L = \frac{L}{\frac{1}{2}\rho v^2 A} = \frac{L}{qA}$$

The quantity one half the density times the velocity squared is called the dynamic pressure  $q$ . The lift coefficient then expresses the ratio of the lift force to the force produced by the dynamic pressure times the area.

## 2.8 Drag force

Drag depends on the density of the air, the square of the velocity, the air's viscosity and compressibility, the size and shape of the body, and the body's inclination to the flow. In general, the dependence on body shape, inclination, air viscosity, and compressibility is very complex.

One way to deal with complex dependencies is to characterize the dependence by a single variable. For drag, this variable is called the drag coefficient, designated "Cd." This allows collecting all the effects, simple and complex, into a single equation. The drag equation states that drag  $D$  is equal to the drag coefficient  $C_d$  times the density times half of the velocity  $V$  squared times the reference area  $A$ .

$$F_D = \frac{1}{2} \rho v^2 C_d A,$$

For given air conditions, shape, and inclination of the object, we must determine a value for  $C_d$  to determine drag. The drag coefficient is a number that aerodynamicists use to model all of the complex dependencies of shape, inclination, and flow conditions on aircraft drag. This equation is simply a rearrangement of the drag equation where we solve for the drag coefficient in terms of the other variables. The drag coefficient  $C_d$  is equal to the drag  $D$  divided by the quantity: density  $\rho$  times half the velocity  $V$  squared times the reference area  $A$ .

$$C_d = \frac{F_d}{\frac{1}{2} \rho v^2 A},$$

The drag coefficient then expresses the ratio of the drag force to the force produced by the dynamic pressure times the area.

## CHAPTER 3

### METHODOLOGY

#### 3.1 Procedure identification

The main task in this project is to study the flow characteristics of the bluff body cut for a square cylinder. The cutting angles used were  $0^\circ$ ,  $30^\circ$  and  $45^\circ$ . The turning angles for each of the cutting angles also vary which are  $0^\circ$ ,  $15^\circ$  and  $285^\circ$ . It focuses on 2 Dimensional planes. This characteristic of the cutting and turning of the bluff body cut will be varied. Simulation by using computational fluid dynamics (CFD) software which is GAMBIT and FLUENT program will shows the different characteristics between them which are drag and lift coefficient.

#### 3.2 Key milestone

The key milestones are listed as below:

1. Identify cutting and rotation angle for square cylinder.
2. Construct the geometrical model for square cylinder using GAMBIT for various cutting and rotation angle.
3. Construct geometric and meshing in GAMBIT which is the pre-processor for FLUENT.
4. Read the mesh into FLUENT.
5. Identify the material which is fluid properties.
6. Study the flow characteristics and verify the characteristics that will be vary according to the different cutting angle and rotation.

### 3.3 The project flow

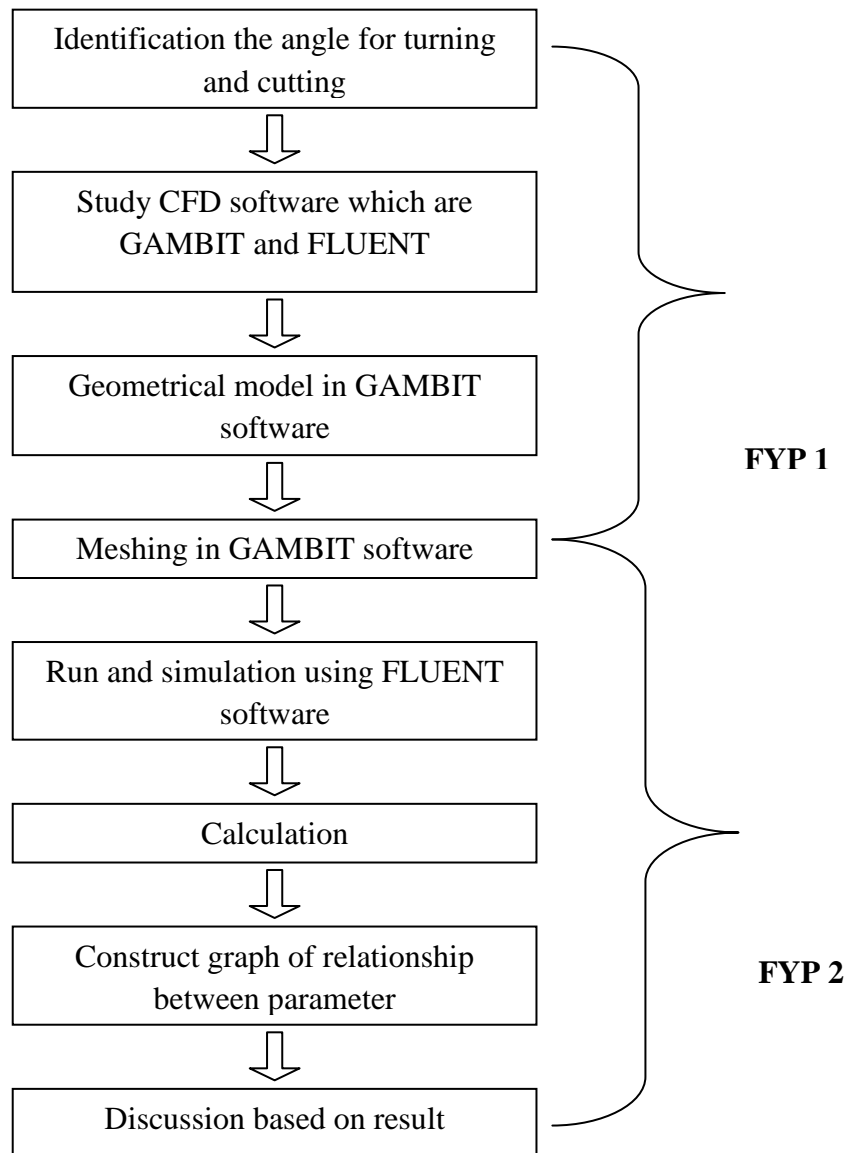


Figure 4: Project Flow

### 3.4 Project Activities

#### 3.4.1 Modeling Using GAMBIT

All the drawing will be done using GAMBIT. There will be 9 designs of different cutting and turning angle. The cutting angles are  $0^\circ$ ,  $30^\circ$  and  $40^\circ$  while the turning angles for each of the cutting angles also vary which are  $0^\circ$ ,  $15^\circ$  and  $285^\circ$

clockwise. The flow characteristics will focus on 2 Dimensional planes for different cutting and rotation angle.

The modeling has to construct in a proper way so it can be mesh using the same software. It can automatically mesh surface and allowing controlling the mesh through the use of sizing functions and boundary layer meshing. Then, the file is exported to FLUENT.

### **3.4.2 Specifying the problem and run the model using FLUENT**

After the model has been generated, boundary condition, medium used is specified so that the simulation could be initiated. Assumption used for are:

- Incompressible flow in two-dimensional geometry with constant fluid properties is assumed. Incompressible flow means, the density of the fluid does not change by an increase in pressure.
- Isothermal flow which fluid remains in the same temperature.
- Fluid is considered homogenous from the standpoint of mass because its density is uniform throughout.
- Fluid is assumed Newtonian fluid, because it continues to display fluid properties no matter how much it is stirred or mixed.
- Fluid is assumed inviscid since the fluid is air. Air having a lower viscosity.
- Steady-state flow which is refers to the condition where the fluid properties at a point in the system do not change over time.
- Fluid is assumed laminar flow, sometimes known as streamline flow, occurs when a fluid flows in parallel layers, with no disruption between the layers.

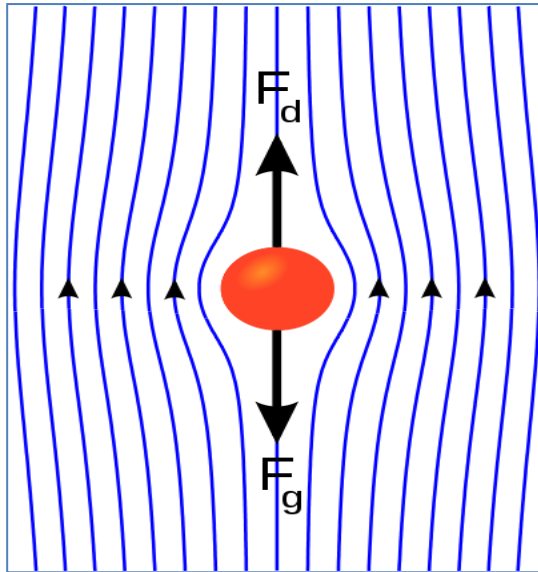


Figure 5: Laminar flow

- The boundary condition included no slip at the square cylinder wall.
- Inlet velocity is assumed 0.25 m/s.
- Pressure outlet is assumed 0 pascal.
- Material of square cylinder is aluminum.
- Simulation using FLUENT: Contour of total pressure.

### 3.4.3 Construct the graph of relationship between parameters

After the simulation is done, some pattern of relationship between the parameters study is plot into graph so that the relationship between them is clear. E.g graph variation of drag coefficient with cylinder orientation for cutting angles  $0^\circ$ ,  $30^\circ$  and  $45^\circ$ .

### 3.4.4 Discussion

The result is then discussed and compare with different cutting and rotation angle. The right explanation is required to justify the result.



### **3.5 Gantt Chart**

For the detail timeline of the project, please refer to *Appendix 9 and 10: Gant Chart*.

### **3.6 Tools and Equipment Needed**

The tools and equipment which are required in this Final Year Project are a Windows based PC together with the programs such as Microsoft Office, GAMBIT and FLUENT which is used to analyze the parameters and produce the related graph, 2 Dimensional model.

## CHAPTER 4

### RESULTS AND DISCUSSION

#### 4.1 Properties of Fluid and Square Cylinder

Fluid that been used is air. This fluid can be assumed as inviscid flow since there are small values for viscosity. The properties of the fluid can be choosing through the FLUENT software. Tables below show properties of air:

Property	Value
Density	1.225 kg/m <sup>3</sup>
Cp (Specific Heat)	1006.43 J/kg-k
Thermal Conductivity	0.0242 W/m-k
Viscosity	1.7894001e-05 kg/m-s
Molecular Weight	28.966 kg/kgmol

Table 1: Data properties of fluid which is air

From the properties of the fluid flow, the Reynolds number can be calculated. Reynolds number will indicate that the flow is the laminar or turbulent flow. However, for this project the flow is determine to be a laminar flow since CFD handle laminar flow with ease but turbulent flow of practical engineering interest are impossible to solve without invoking turbulence model.

The factor that determines which type of flow is present is the ratio of inertia forces to viscous forces within the fluid, expressed by the non dimensional Reynolds Number,

$$R = \frac{\rho VD}{\mu}$$

where  $V$  and  $D$  are a fluid characteristic velocity and distance.  $V$  is for the initial velocity of the boundary flow while  $D$  for the diameter of boundary flows.

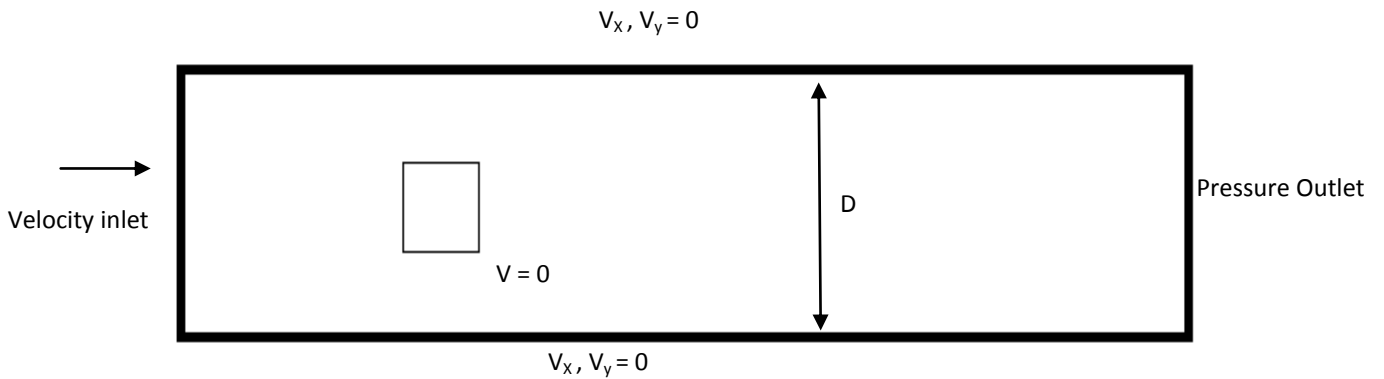


Figure 6: Fluid Flow for Square Cylinder

Fluid flows are laminar for Reynolds Numbers up to 2000. For this project, flow is assumed to be laminar. As of FLUENT simulation, we assume the velocity inlet is constant which are 0.25 m/s.

#### 4.2 Cutting and Rotation Angle for Square Cylinder

Square cylinder will be cut to study the flow characteristics by numerical using GAMBIT and FLUENT software. The bluff body cut for the different cutting are been rotate with the  $15^{\circ}$  clockwise angle and  $75^{\circ}$  counter clockwise angles. The cutting and rotation of the body are been doing using GAMBIT. The cutting angles are  $0^{\circ}$ ,  $30^{\circ}$  and  $45^{\circ}$ . The flow characteristics will focus on 2 Dimensional planes for different cutting and rotation angle.

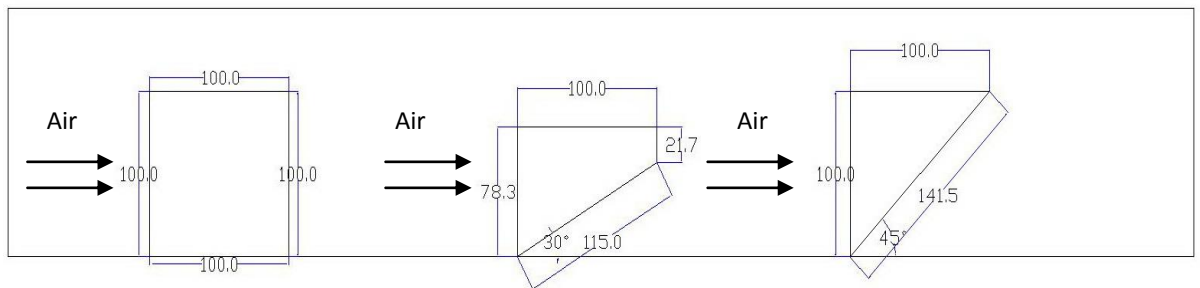


Figure 7: Different Cutting Angles which are,  $0^{\circ}$ ,  $30^{\circ}$  and  $45^{\circ}$

#### **4.2.1 Analysis Using GAMBIT**

Geometrical model and meshing had been done using GAMBIT. Boundary condition also was specifying to export the file from GAMBIT to FLUENT software. FLUENT will solve the problem and show the characteristics for each cutting and turning angle of square block.

Firstly, create the geometry for the boundary flow which is the rectangle shape. In order to create the rectangle, first create the vertices at the four corners. The vertices are (0,-3), (0, 3), (20, 3) and (20,-3). Join the adjacent vertices by straight lines to form the edges of the rectangle. Then, create geometry of the square shape in the rectangle shape. The vertices had been joining to form edges.

After that, faces had been create corresponding to the area enclosed by the edges. There are two faces been created which are one for the rectangle which is fluid boundary and another one for the square block. However the rectangle shape will be subscribe the square shape. So, the faces will become one. Since the problem in 2D, it is not needed to form a "volume" from faces. So the hierarchy of geometric objects in GAMBIT is vertices -> edges -> faces -> volumes.

Meshing is been done on the rectangular subscribe the square face with 0.25 interval size. Then set the boundary types in GAMBIT. For the rectangle, the left edge is the inlet of the boundary; the right edge the outlet, the top and bottom edges are the wall. However, for all of the edges of square cylinder is interface. These steps are been repeated using different cutting and rotation angle.

#### **4.2.2 Analysis Using FLUENT**

Once FLUENT is loaded, select 2ddp from the list option. Option "2ddp" is used to select 2-dimensional, double-precision solver. Then, read the case of msh file. FLUENT will tell the mesh statistics as it reads in the mesh. Grid must been check to make sure that there are no errors. A display window will show the grid to give a visual check on the boundary conditions.

As the grid is correct, properties of the problem must be defined. The three crucial categories under Define are Models, Materials and Boundary Condition. After that, look up at solution parameters. Keep an eye on the iteration as it does converge to the solution. Solution of vector, contour and XY plot are been display.

### **4.3 Simulation Model**

All the model must be solving using FLUENT. Inevitably any iterative/numerical solution procedure will only give a solution which is “converged” relative to some criteria. The solution may be converged if:

- All discretized transport equations are obeyed to a specified tolerance defined by Fluent’s residuals
- The solution no longer changes with more iterations
- Overall balances close

### **4.4 0° Cutting Model**

#### **4.4.1 0° Rotation Model**

In FLUENT, the condition for 0° cutting and rotation is then been set and the reading is taken from 118 iterations since the solution is converged.

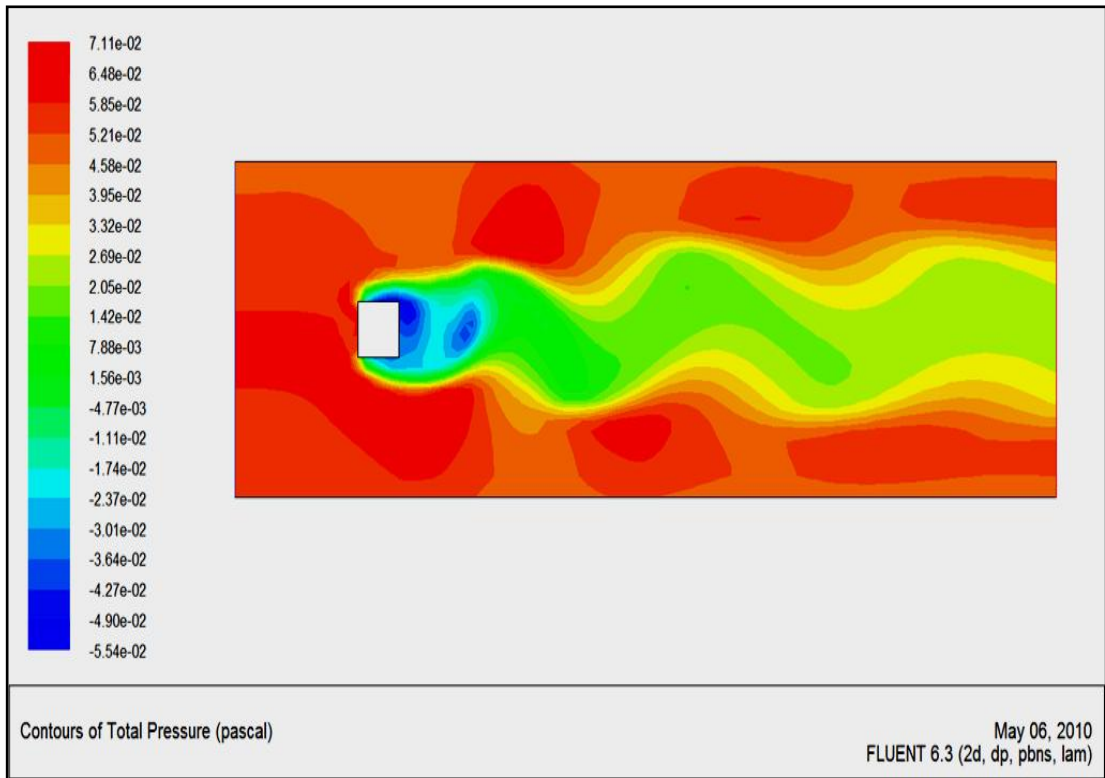


Figure 8: Contour of total pressure of  $0^{\circ}$  cutting and  $0^{\circ}$  rotation

Contour of total pressure shows that the upper and lower flow has the high total pressure. The circulation of lower flow which is  $-5.54e-02$  can be seen behind the square cylinder. The flow is been block by the cylinder, and the flow after the blockage keep increasing into the pressure outlet.

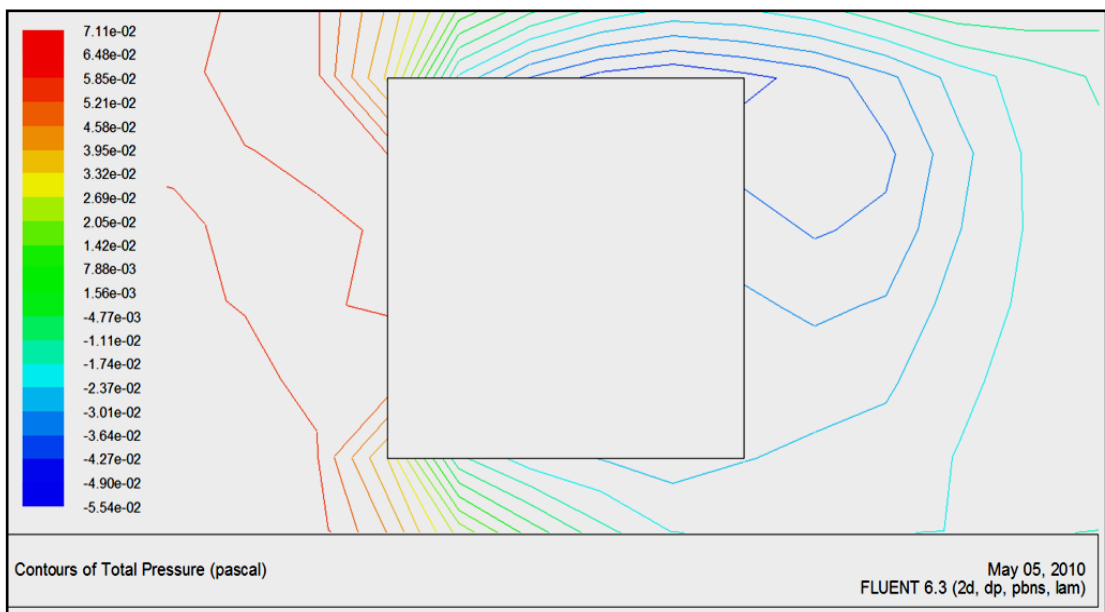


Figure 9: Contour of total pressure of  $0^{\circ}$  cutting and  $0^{\circ}$  rotation square block

There are 36 points of total pressure. From total pressure, calculate pressure in x and y-direction to determine drag and lift force. Table for total pressure is been attach in appendix 1.

From table:

$$\text{Drag force} = \text{Force in x- direction} = P_x \times d_y = 1.0E-02$$

$$\text{Lift force} = \text{Force in y- direction} = P_y \times d_x = -2.9E-04$$

#### 4.4.2 15° Clockwise Rotation Model

In FLUENT, the condition for 0° cutting and 15° clockwise rotations is then been set and the reading is taken from 104 iterations since the solution is converged.

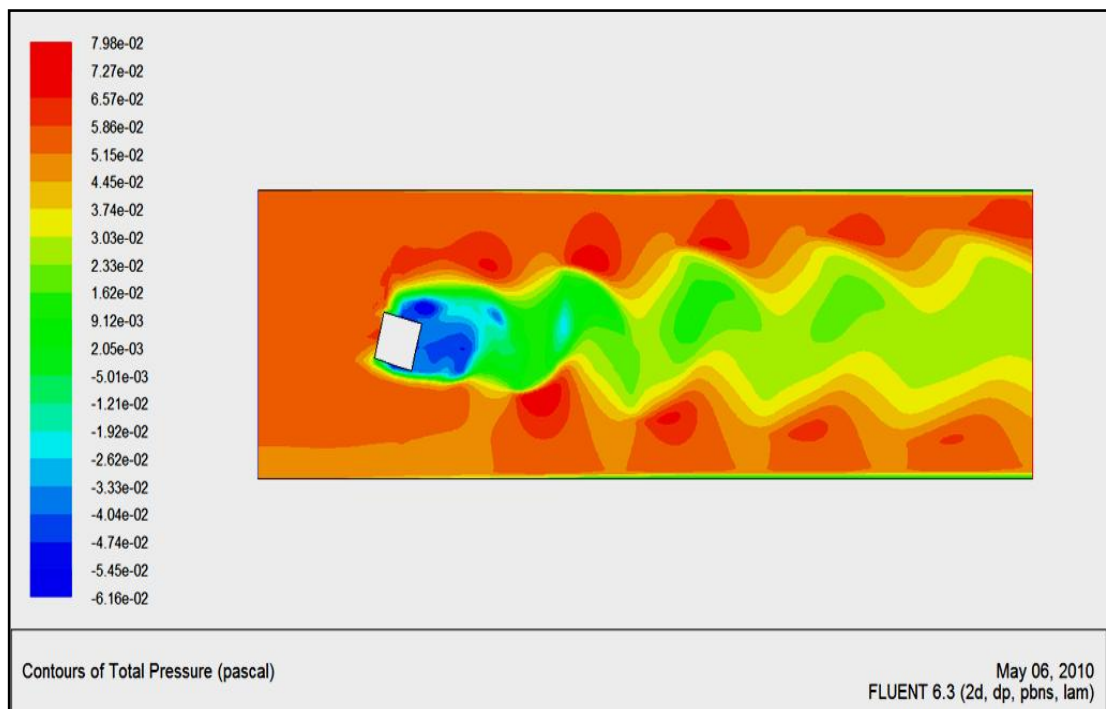
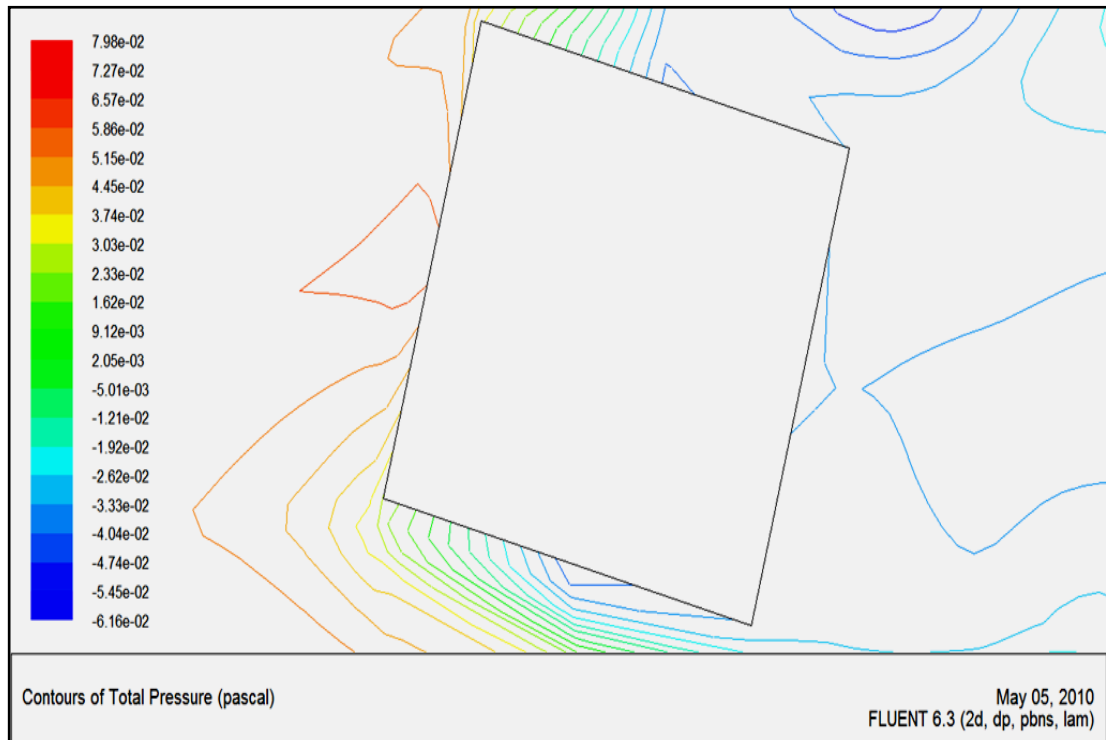


Figure 10: Contour of total pressure of 15° clockwise rotation

Contour of total pressure shows that the upper and lower flow has the high total pressure. The circulation of lower flow which is  $-6.16e-02$  can be seen behind the square cylinder. The flow is been block by the cylinder, and the flow after the

blockage keep increasing into the pressure outlet. The circulation of highest total pressure can be seen next to the flow that been blockage from cylinder.



**Figure 11: Contour of total pressure of 15° clockwise rotation square block**

There are 38 points of total pressure. From total pressure, calculate pressure in x and y-direction to determine drag and lift force. Table for total pressure is been attach in appendix 2.

From table:

$$\text{Drag force} = \text{Force in x- direction} = P_x \times d_y = 2.13\text{E-}03$$

$$\text{Lift force} = \text{Force in y- direction} = P_y \times d_x = 8.30\text{E-}04$$



#### 4.4.3 285° Clockwise Rotation Model

In FLUENT, the condition for 0° cutting and 285° clockwise rotations is then been set and the reading is taken from 80 iterations since the solution is converged.

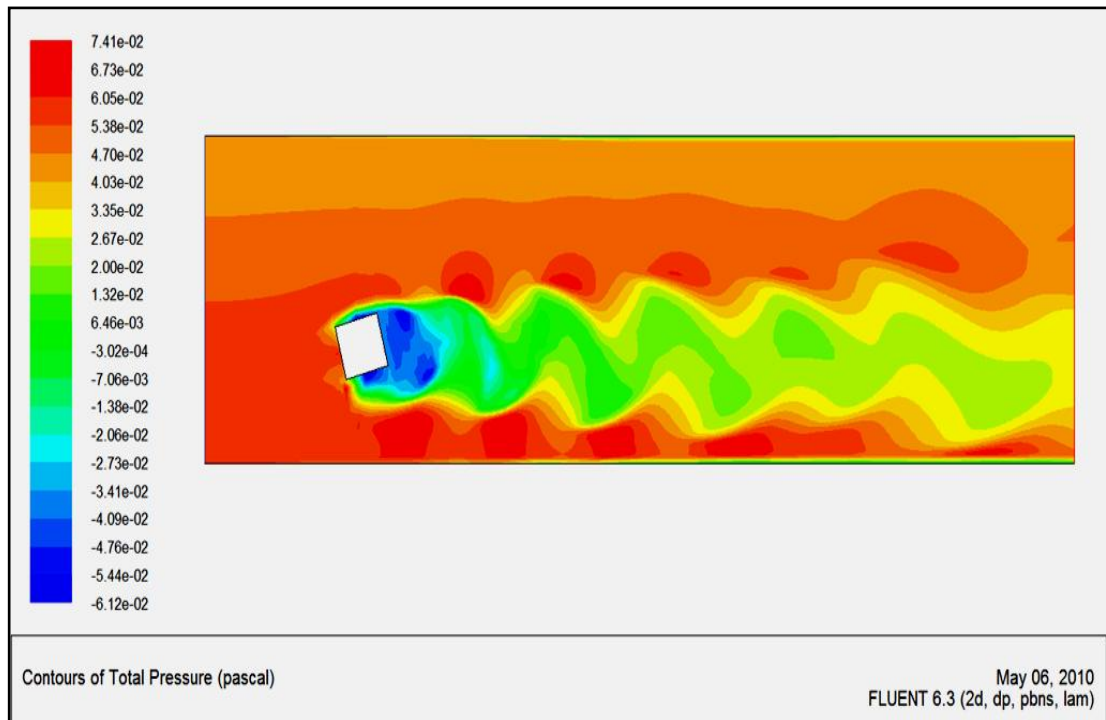


**Figure 12: Contour of total pressure of 285° clockwise rotation**

Contour of total pressure shows that flow has the high total pressure at the front of the cylinder. The circulation of lower flow which is  $-6.12 \times 10^{-2}$  can be seen behind the square cylinder. The flow is been block by the cylinder, and the flow after the blockage keep increasing into the pressure outlet.



Figure 13: Contour of total pressure of 285<sup>0</sup> clockwise rotation square block

There are 40 points of total pressure. From total pressure, calculate pressure in x and y-direction to determine drag and lift force. Table for total pressure is been attach in appendix 3.

From table:

$$\text{Drag force} = \text{Force in x- direction} = P_x \times d_y = 5.47\text{E-}05$$

$$\text{Lift force} = \text{Force in y- direction} = P_y \times d_x = 2.79\text{E-}03$$

## 4.5 30° Cutting Model

### 4.5.1 0° Rotation Model

In FLUENT, the condition for 30° cutting and 0° rotation is then been set and the reading is taken from 118 iterations since the solution is converged.

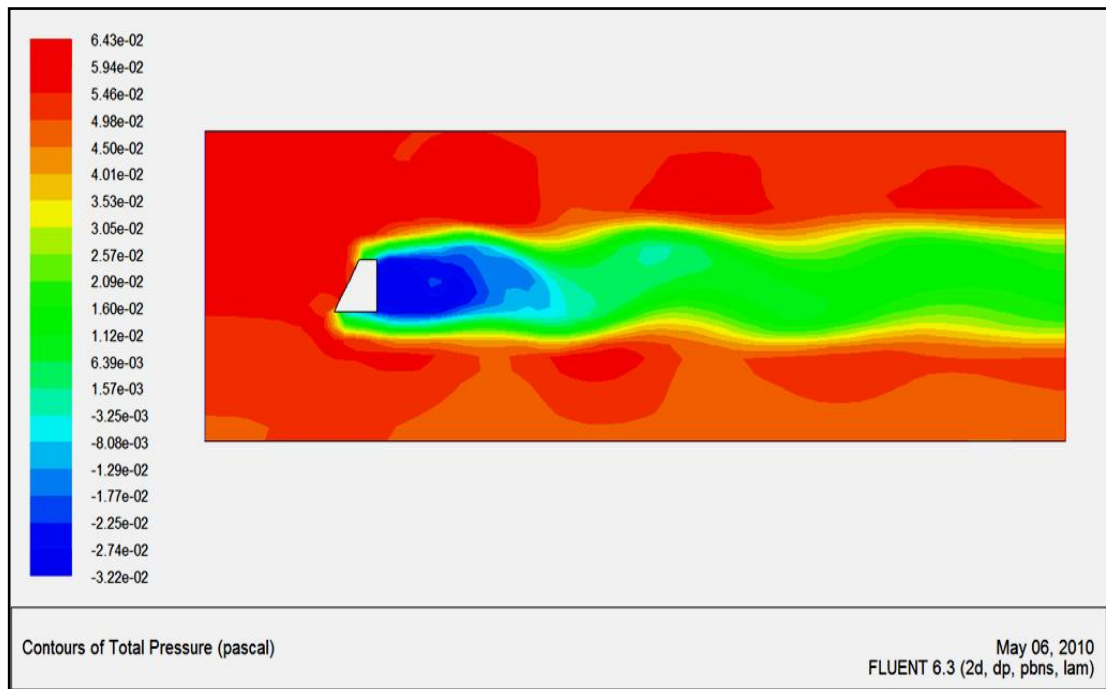


Figure 14: Contour of total pressure of 30° cutting and 0° rotation

Contour of total pressure shows that the upper and lower flow has the high total pressure. The circulation of lower flow which is  $-3.32 \times 10^{-2}$  can be seen behind the square cylinder. The flow is been block by the cylinder, and the flow after the blockage keep increasing into the pressure outlet.

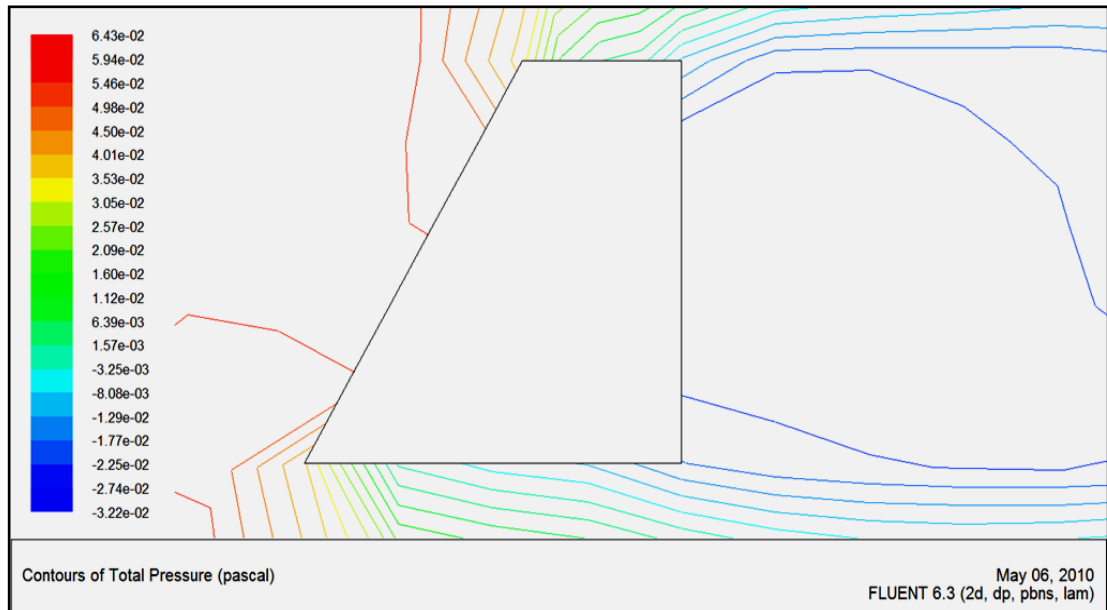


Figure 15: Contour of total pressure of  $30^{\circ}$  cutting and  $0^{\circ}$  rotation square block

There are 36 points of total pressure. From total pressure, calculate pressure in x and y-direction to determine drag and lift force. Table for total pressure is been attach in appendix 4.

From table:

$$\text{Drag force} = \text{Force in x- direction} = P_x \times d_y = 2.39\text{E-}03$$

$$\text{Lift force} = \text{Force in y- direction} = P_y \times d_x = -3.15\text{E-}03$$

## 4.5.2 15° Clockwise Rotation Model

In FLUENT, the condition for 30° cutting and 15° clockwise rotations is then been set and the reading is taken from 180 iterations since the solution is converged.

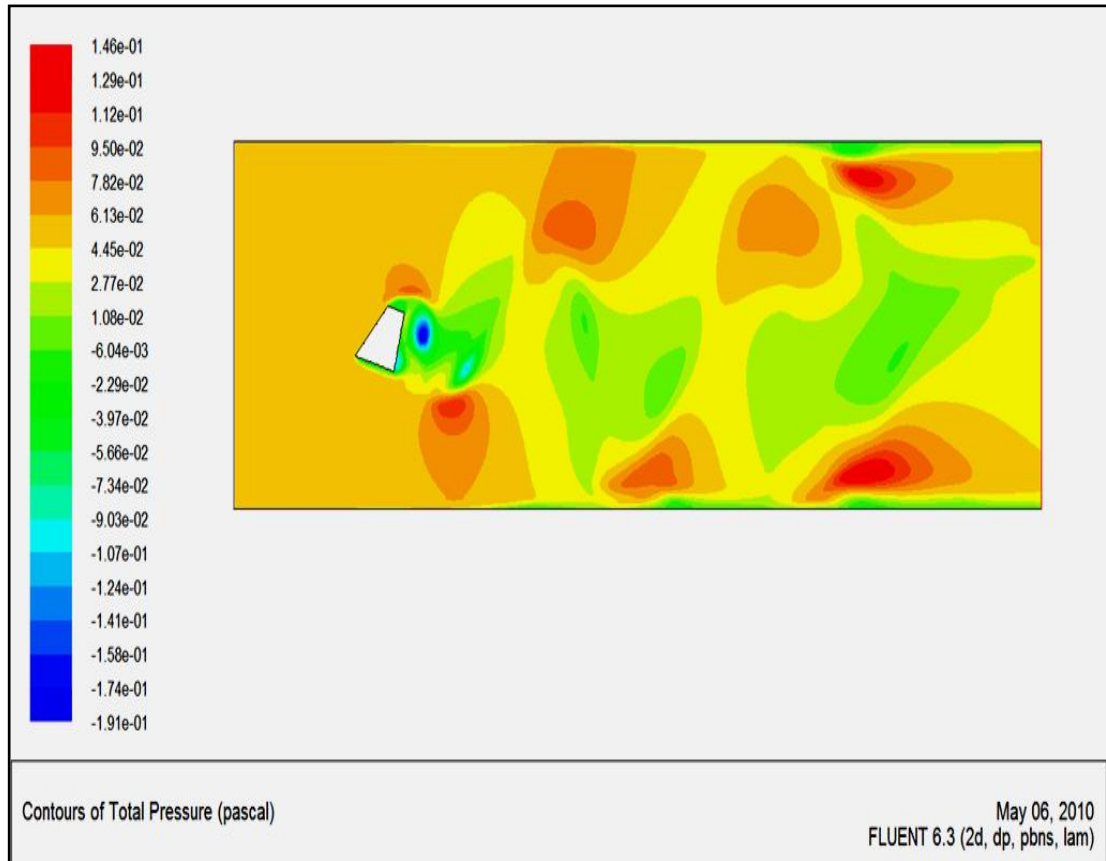
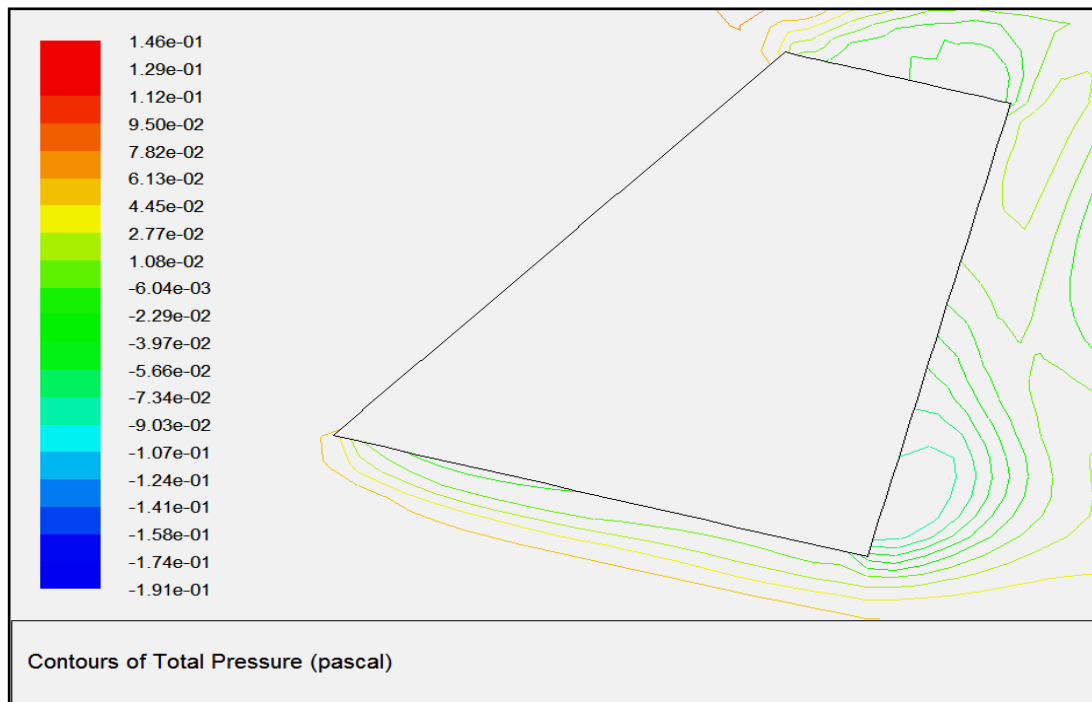


Figure 16: Contour of total pressure of 15° clockwise rotation

Contour of total pressure shows that the upper and lower flow has the high total pressure. The circulation of lower flow which is  $-1.91e-01$  can be seen behind the square cylinder. The flow is been block by the cylinder, and the flow after the blockage keep increasing into the pressure outlet. The circulation of highest total pressure can be seen next to the flow that been blockage from cylinder.



**Figure 17: Contour of total pressure of 15° clockwise rotation square block**

There are 26 points of total pressure. From total pressure, calculate pressure in x and y-direction to determine drag and lift force. Table for total pressure is been attach in appendix 5.

From table:

$$\text{Drag force} = \text{Force in x- direction} = P_x \times d_y = 5.83E-03$$

$$\text{Lift force} = \text{Force in y- direction} = P_y \times d_x = -1.70E-03$$

### 4.5.3 285° Clockwise Rotation Model

In FLUENT, the condition for 30° cutting and 285° clockwise rotations is then been set and the reading is taken from 80 iterations since the solution is converged.

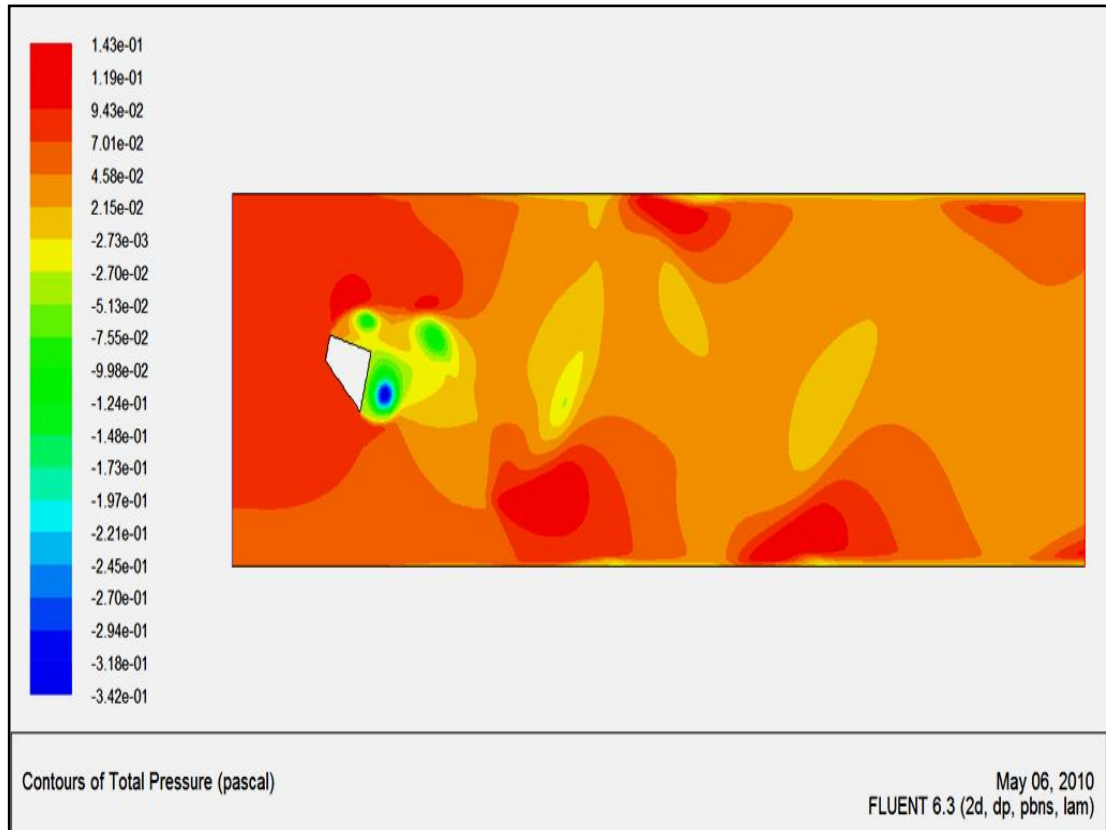


**Figure 18: Contour of total pressure of 285° clockwise rotation**

Contour of total pressure shows that flow has the high total pressure at the front of the cylinder. The circulation of lower flow which is  $-3.42e-01$  can be seen behind the square cylinder. The flow is been block by the cylinder, and the flow after the blockage keep increasing into the pressure outlet.

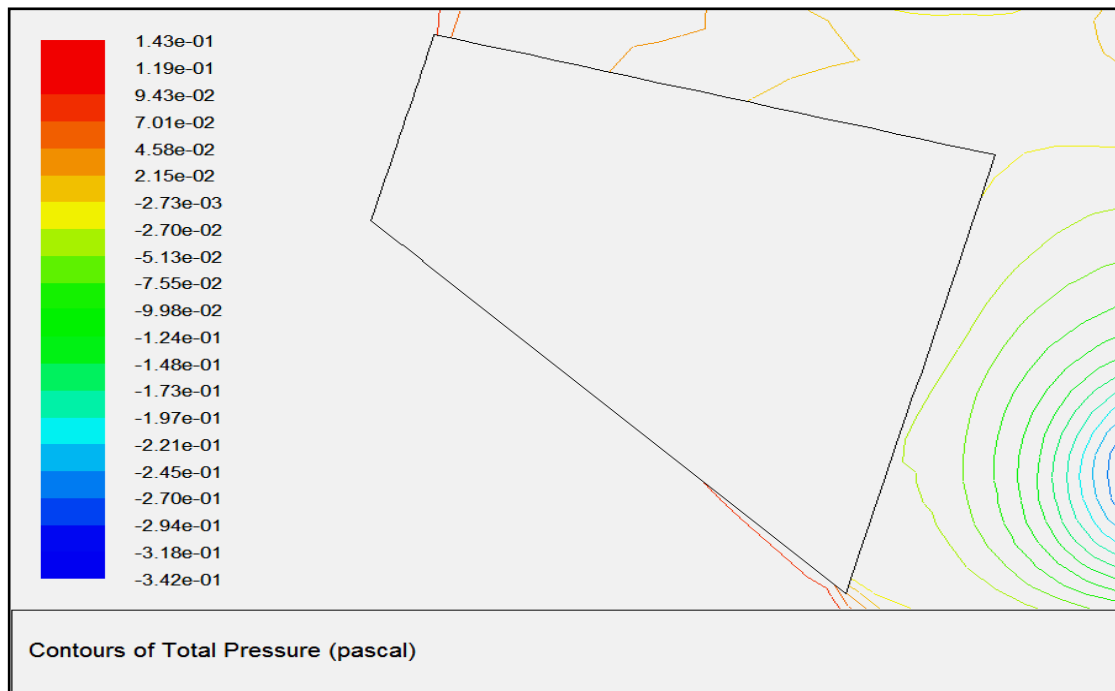


Figure 19: Contour of total pressure of 285<sup>0</sup> clockwise rotation square block

There are 10 points of total pressure. From total pressure, calculate pressure in x and y-direction to determine drag and lift force. Table for total pressure is been attach in appendix 6.

From table:

$$\text{Drag force} = \text{Force in x- direction} = P_x \times d_y = 8.26\text{E-}05$$

$$\text{Lift force} = \text{Force in y- direction} = P_y \times d_x = 2.17\text{E-}03$$



## 4.6 45° Cutting Model

### 4.6.1 0° Rotation Model

In FLUENT, the condition for 45° cutting and 0° rotation is then been set and the reading is taken from 85 iterations since the solution is converged.

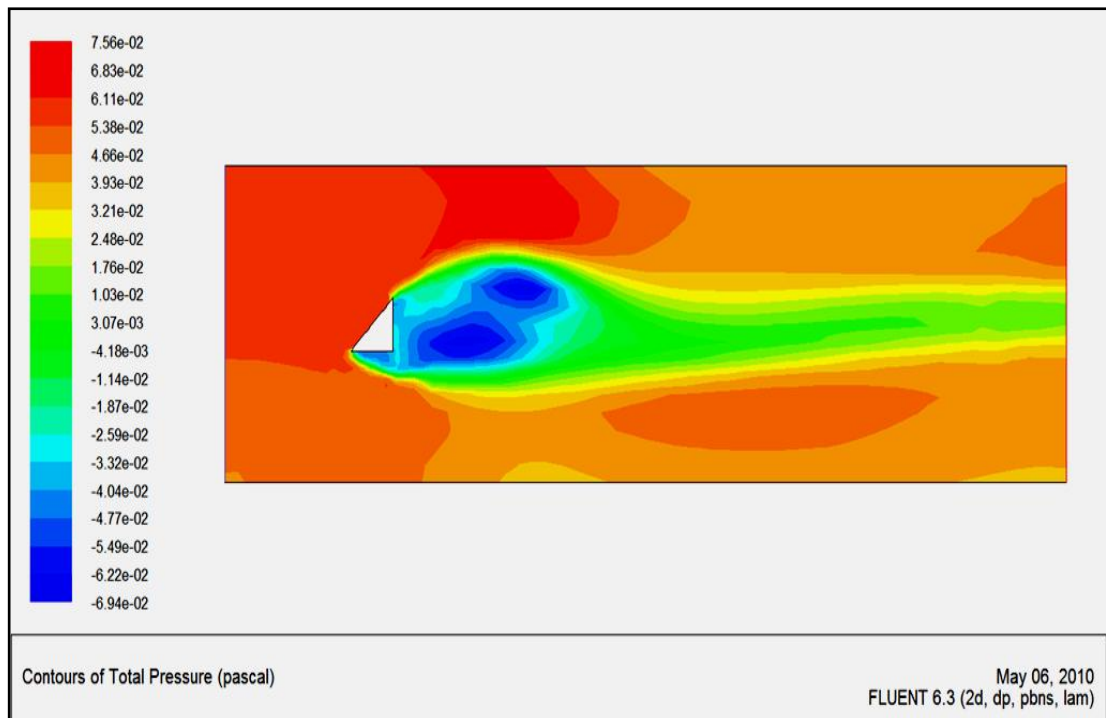


Figure 20: Contour of total pressure of 0° rotation

Contour of total pressure shows that flow has the high total pressure in front of the cylinder. The circulation of lower flow which is -6.94-02 can be seen behind the square cylinder. The flow is been block by the cylinder, and the flow after the blockage keep increasing into the pressure outlet.

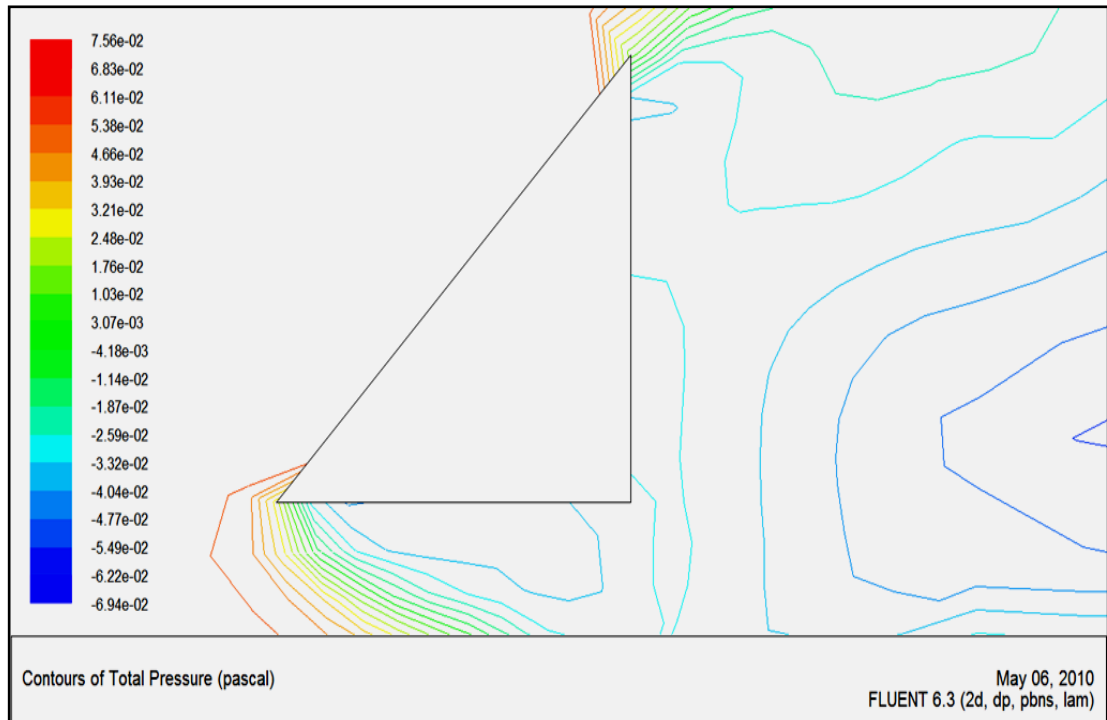


Figure 21: Contour of total pressure of  $45^{\circ}$  cutting and  $0^{\circ}$  rotation square block

There are 31 points of total pressure. From total pressure, calculate pressure in x and y-direction to determine drag and lift force. Table for total pressure is been attach in appendix 7.

From table:

$$\text{Drag force} = \text{Force in x- direction} = P_x \times d_y = 5.00\text{E-}05$$

$$\text{Lift force} = \text{Force in y- direction} = P_y \times d_x = 4.15\text{E-}03$$

#### 4.6.2 15° Clockwise Rotation Model

In FLUENT, the condition for 45° cutting and 15° clockwise rotations is then been set and the reading is taken from 102 iterations since the solution is converged.

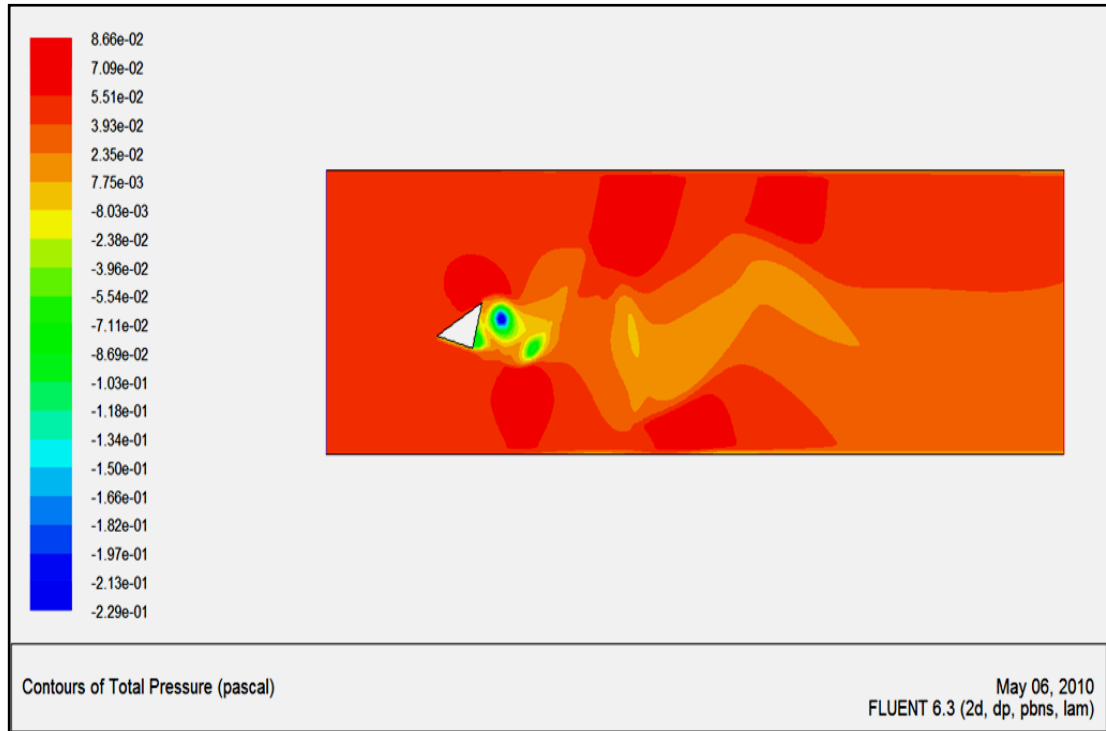


Figure 22: Contour of total pressure of 15° clockwise rotation

Contour of total pressure shows that the upper and lower flow has the high total pressure. The circulation of lower flow which is  $-2.29e-01$  can be seen behind the square cylinder. The flow is been block by the cylinder, and the flow after the blockage keep increasing into the pressure outlet. The circulation of highest total pressure can be seen next to the flow that been blockage from cylinder.

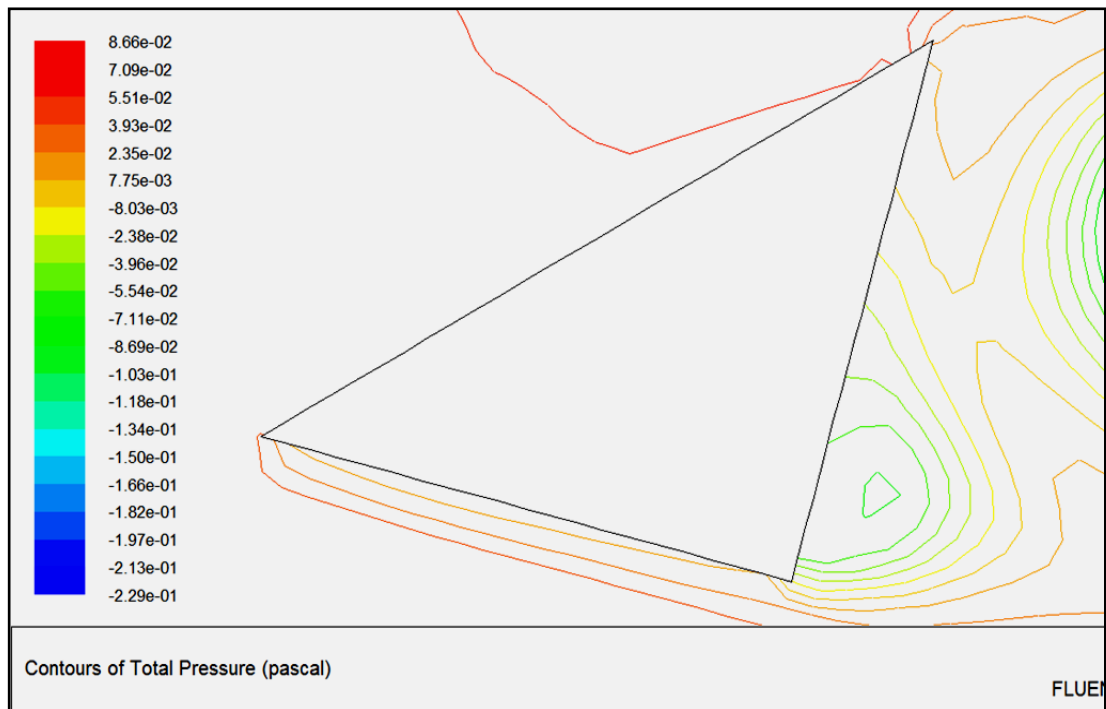


Figure 23: Contour of total pressure of 15° clockwise rotation square block

There are 20 points of total pressure. From total pressure, calculate pressure in x and y-direction to determine drag and lift force. Table for total pressure is been attach in appendix 8.

From table:

$$\text{Drag force} = \text{Force in x- direction} = P_x \times d_y = 4.29\text{E-}05$$

$$\text{Lift force} = \text{Force in y- direction} = P_y \times d_x = -7.15\text{E-}05$$

### 4.6.3 285° Clockwise Rotation Model

In FLUENT, the condition for 45° cutting and 285° clockwise rotations is then been set and the reading is taken from 66 iterations since the solution is converged.

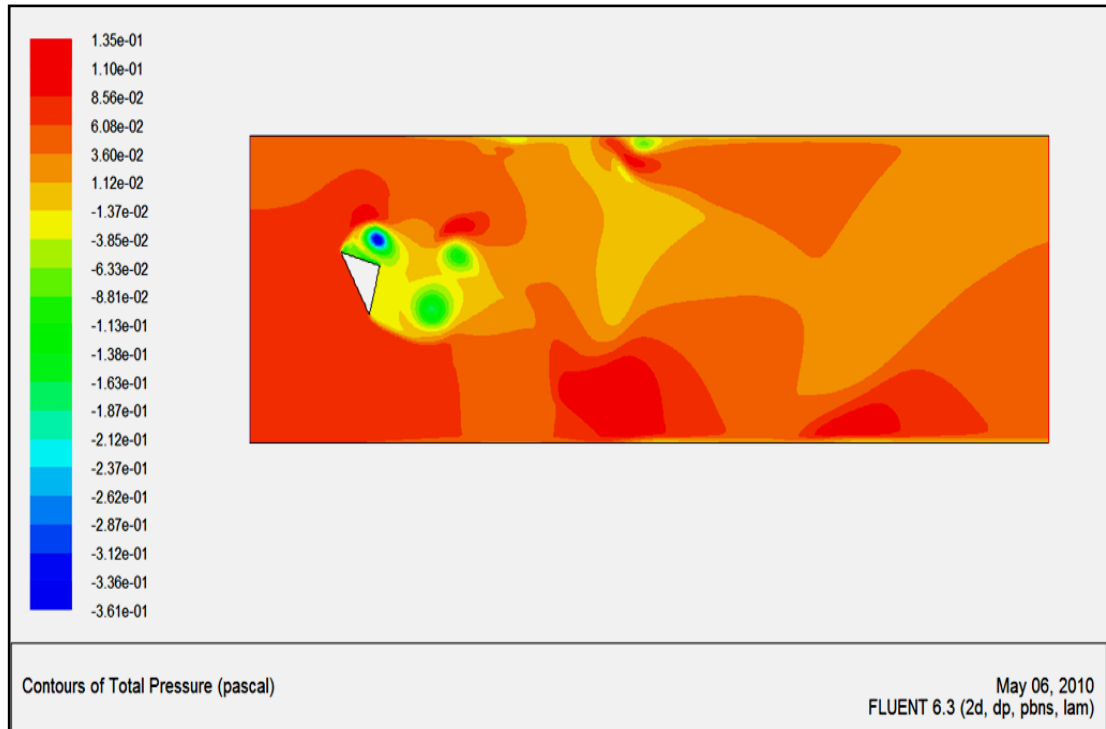


Figure 24: Contour of total pressure of 285° clockwise rotation

Contour of total pressure shows that the flow has the high total pressure in front of the cylinder. The circulation of lower flow which is  $-3.616e-01$  can be seen behind the square cylinder. The flow is been block by the cylinder, and the flow after the blockage keep increasing into the pressure outlet. The circulation of highest total pressure can be seen next to the flow that been blockage from cylinder.

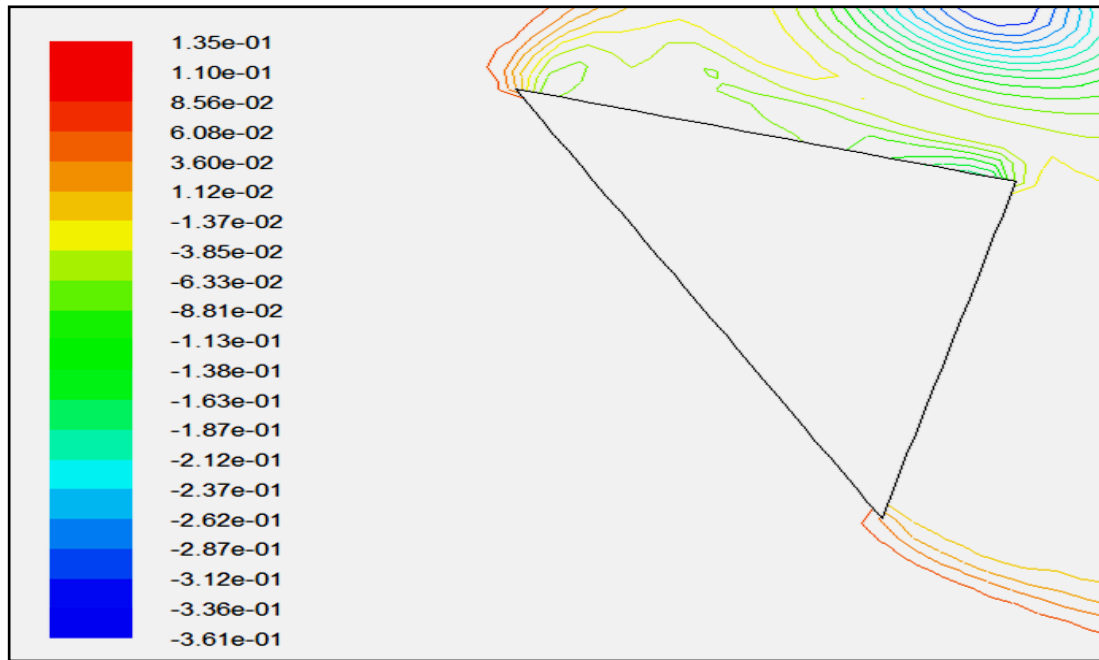


Figure 25: Contour of total pressure of 285<sup>0</sup> clockwise rotation square block

There are 23 points of total pressure. From total pressure, calculate pressure in x and y-direction to determine drag and lift force. Table for total pressure is been attach in appendix 9.

From table:

$$\text{Drag force} = \text{Force in x- direction} = P_x \times d_y = 1.25\text{E-}02$$

$$\text{Lift force} = \text{Force in y- direction} = P_y \times d_x = -9.80\text{E-}03$$

## 4.7 Discussion

Lift is defined to be the component of this force that is perpendicular to the incoming flow direction. It contrasts with the drag force, which is defined to be the component of the surface force parallel to the flow direction. So, lift force is the flow in y-direction while drag force is the force in x-direction.

Force depends on the fluid pressure, multiplied by the surface area used to face the pressure. FLUENT will show the contours of total pressure. From total pressure, pressure in x and y- direction can be calculated by determine the angle of total pressure.

Lift force can be determined by multiply pressure in y-direction with displacement of the point. While drag force can be determined by multiply pressure in x-direction with displacement of the point. Displacement can be assumed to be area since the length is 1. Thus, displacement is multiplied by 1 to get the area.

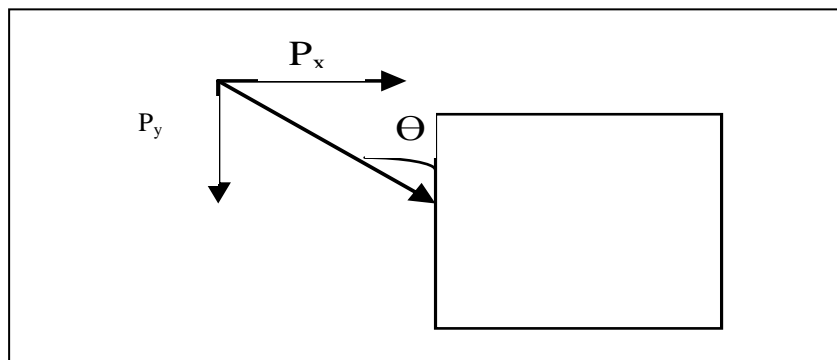


Figure 26: Pressure in x and y-direction

cutting	rotation	drag force (N)	lift force (N)	drag coefficient	lift coefficient
0 <sup>0</sup>	0 <sup>0</sup>	0.010173	-0.000289	2.657515	-0.075366
	15 <sup>0</sup>	0.002135	0.000830	0.557692	0.216834
	285 <sup>0</sup>	0.000055	0.002791	0.014284	0.729108
30 <sup>0</sup>	0 <sup>0</sup>	0.002389	-0.003152	0.624190	-0.823316
	15 <sup>0</sup>	0.005826	-0.001695	1.521872	-0.442868
	285 <sup>0</sup>	0.000083	0.002168	0.021571	0.566240
45 <sup>0</sup>	0 <sup>0</sup>	0.000050	0.004153	0.013073	1.084863
	15 <sup>0</sup>	0.000043	-0.000071	0.011215	-0.018672
	285 <sup>0</sup>	0.012501	-0.009795	3.265561	-2.558728

Table 2: List of lift and drag force and coefficient

From the table 2 above, it shows that drag and lift coefficient can be calculated using drag and lift force. Drag and lift coefficient can be calculated by using the equation below:

Lift coefficient:

$$C_L = \frac{F_y}{\frac{1}{2}\rho v^2 A}$$

Drag coefficient:

$$C_D = \frac{F_x}{\frac{1}{2}\rho v^2 A}$$



It is same for  $\rho, v$  and  $A$  for every cutting and rotation.

$$\rho = 1.225 \text{ kg/m}^3$$

$$v = 0.25 \text{ m/s}$$

$$A = 0.1 \text{ m}^2$$

Example for  $0^\circ$  cutting and  $0^\circ$  rotations:

$$C_L = \frac{F_y}{\frac{1}{2}\rho v^2 A} = \frac{-2.9\text{E} - 04}{\frac{1}{2} 1.225(0.25^2)0.1}$$

$$= -0.075366$$

$$C_D = \frac{F_x}{\frac{1}{2}\rho v^2 A} = \frac{8.30\text{E} - 04}{\frac{1}{2} 1.225(0.25^2)0.1}$$

$$= -0.075366$$

This table shows that a model with  $45^\circ$  cutting and  $285^\circ$  clockwise rotation give the highest drag coefficient. Shape has a very large effect on the amount of drag produced. The drag on a sphere is highly dependent on Reynolds number. Flow past a cylinder, goes through a number of transitions with velocity. At very low velocity which is at the inlet velocity, stable pair of vortices is formed on the downwind side.

As velocity increases, the vortices become unstable and are alternately shed downstream. As velocity is increased even more, the boundary layer transitions to chaotic turbulent flow with vortices of many different scales being shed in a turbulent wake from the body. It can be seen from the contour of total pressure. Each of these flow regimes produces a different amount of drag on the sphere. The downstream shape can be modified to reduce drag [13].

A model with  $45^\circ$  cutting and  $15^\circ$  clockwise rotation has the lowest drag and lift coefficient. The main reason for a minimum in drag coefficient is wake asymmetry

originating from shear layers of unequal length on each side of the cylinder. The loss of symmetry of the wake increases the base pressure, and lowers drag. Lower drag coefficient indicates the object will have less aerodynamic or hydrodynamic drag.

Aerodynamic effects represent a substantial fraction of the energy. It is also a factor in building design, where low drag, coupled with reduced lift, results in a structure which can achieve stability. For building structure, it is also needed to have low lift coefficient in order to be more stable. However high lift airfoils are advantageous on aircraft, where a higher wing loading provides better cruise performance [14].

Even though a model with  $45^\circ$  cutting has the lowest lift force, it also experienced the highest lift force for  $0^\circ$  rotation.

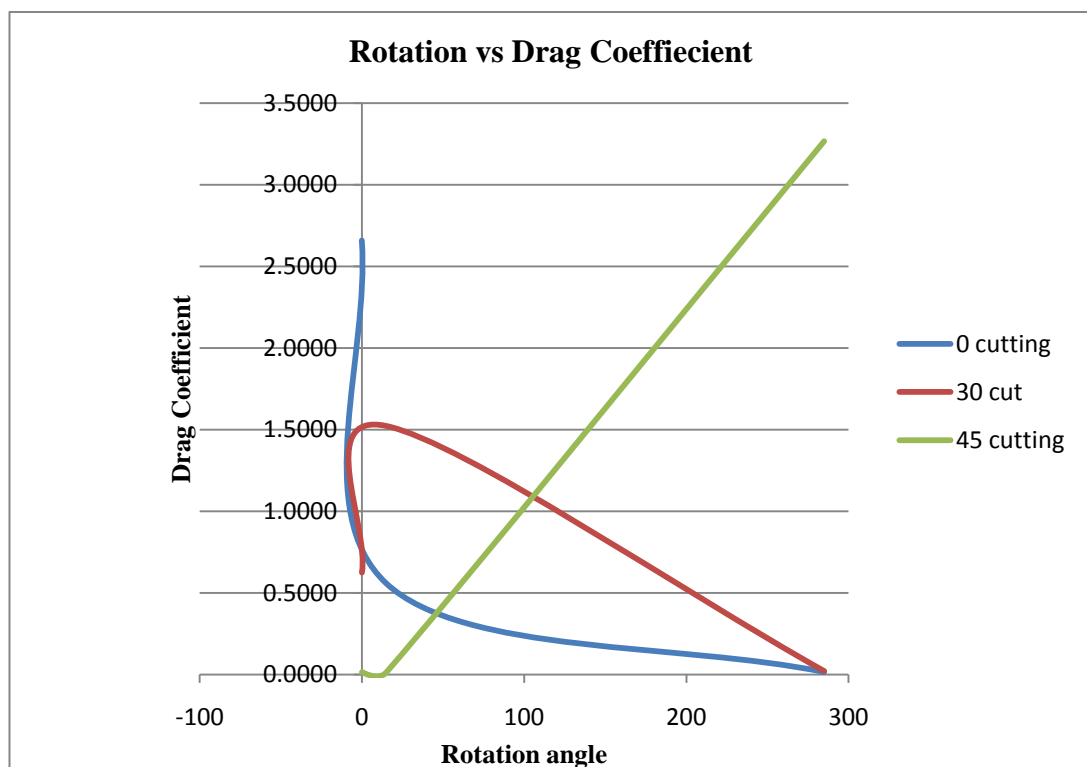


Figure 27: Rotation vs Drag Coefficient

According to the figure 27, model with  $45^\circ$  cutting has the lowest drag coefficient at  $15^\circ$  clockwise rotation angles. While for  $0^\circ$  and  $30^\circ$  cutting has lowest drag coefficient at  $285^\circ$  clockwise rotation angle. The model of  $45^\circ$  cutting has the highest

drag coefficient compare to other model. Drag coefficient for  $45^{\circ}$  cutting model is keep increasing with the increasing of the rotation angle. It can be conclude that cutting and rotation angle will affect drag coefficient. Drag coefficient can be increasing by increasing the cutting and rotation angle.

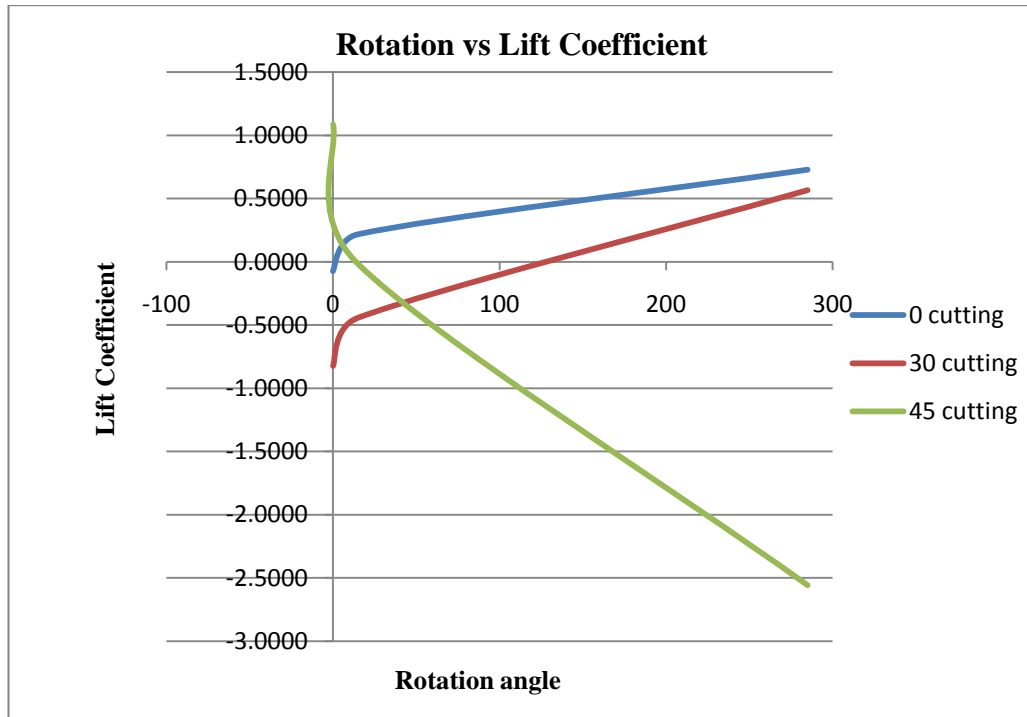


Figure 28: Rotation vs Lift Coefficient

Based from the figure 28, lowest lift coefficient can be get from the  $45^{\circ}$  cutting model with increasing the rotation angle. Lift coefficient for  $45^{\circ}$  cutting model decreasing to negative value. The lift due to pressure was negative (downward), while the lift due to friction was positive. Graph for  $0^{\circ}$  and  $30^{\circ}$  cutting model are slightly the same. Lift coefficient for  $0^{\circ}$  and  $30^{\circ}$  cutting models are increasing with the increasing of the rotation angle.

## **CHAPTER 5**

### **CONCLUSION AND RECOMMENDATION**

#### **5.1 Conclusion**

As a conclusion, this project is carried out to study the flow characteristics for cutting and rotating angle on the bluff body cut for a square cylinder using numerical method.

The methodology which is used in this project can support the objectives in the project which are geometrical modeling and meshing using GAMBIT while the solver to show the characteristics by using FLUENT.

Geometrical modeling and meshing for each cutting and rotation angle will be carried out using GAMBIT. Then, the meshing will be solving using FLUENT. The solver will show the characteristics. Drag and lift coefficient is calculated based on simulation from FLUENT

#### **5.2 RECOMMENDATION**

1. Increase the number of meshing for a finer and better analysis.
2. 3 Dimensional investigations will improve the study since the height of the cylinder also been considered. It would give better picture on the characteristics.
3. Increase the number of iterations applied to the solver. This could help ones getting more accurate result. The only thing limiting this is the capability of the computer itself.
4. Study other characteristics of the flow such as time average velocity profile and vorticity field of the flow.

## REFERENCES

- [1] L. Skerget & J. Ravnik, 2007, "Flow over a square cylinder by BEM" in C.A. Brebbia *Boundary Elements and Other Mesh Reduction Methods XXIX*, Wessex Institute of Technology, UK, D. Poljak, University of Split, Croatia and V. POPOV, Wessex Institute of Technology, UK
  
- [2] A. K. Saha, K. Muralidhar, And G. Biswas, 2000, "Transition And Chaos In Two-Dimensional Flow Past A Square Cylinder," *Journal of Engineering Mechanics*, Vol. 126, No. 5, pp. 523-532
  
- [3] Astu Pudjanarsa, 2006, "Experimental study on the effect of turning angle on drag and lift forces for various cut angles on spheres" *Proc. IMechE Vol. 221 Part C: J. Mechanical Engineering Science*
  
- [4] Yunus A. Cengel and John M. Cimbala, 2004, *Fluid Mechanics*, Mcgraw-Hill Series in Mechanical Engineering
  
- [5] A. K. Saha, K. Muralidhar, And G. Biswas, 1999, "Vortex structures and kinetic energy budget in two-dimensional flow past a square cylinder" *Journal of Engineering Mechanics*, Vol. 126, No. 5, pp. 523-532
  
- [6] S. Aiba and H. Watanabe, 1997, "Flow Characteristics of a Bluff Body Cut From a Circular Cylinder" *Journal of Fluids Engineering*, Vol. 119/453
  
- [7] Jyoti Chakraborty, Nishith Verma and R. P. Chhabra, 2004, "Wall effects in flow past a circular cylinder in a plane channel: a numerical study" *Chemical Engineering and Processing*, Volume 43, Issue 12, pp. 1529-1537
  
- [8] Shuyang Cao and Yukio Tamura; 2008, "Flow around a circular cylinder in linear shear flows at subcritical Reynolds number" *Journal of Wind Engineering and Industrial Aerodynamics* 96

- [9] Sumeet Thete, Kaustubh Bhat and M. R. Nandgaonkar, 2009, “2D Numerical Simulation of Fluid Flow over a Rectangular Prism” *ISSR Journal*, Vol. 1 (1)
- [10] A. Sohankar, C. Norberg and L. Davidson, 1998, “Low-Reynolds-Number Flow around A Square Cylinder at Incidence: Study of Blockage, Onset of Vortex Shedding and Outlet Boundary Condition” *International Journal for Numerical Methods in Fluids*, Vol. 26 (39-56)
- [11] Sushanta Dutta, P. K. Panigrahi and K. Muralidhar, 2008 “Experimental Investigation of Flow past a Square Cylinder at an Angle of Incidence” *Journal Of Engineering Mechanics*
- [12] <http://courses.cit.cornell.edu/fluent/#what>
- [13] <http://www.grc.nasa.gov/WWW/K-12/airplane/shaped.html>
- [14] <http://www.orienttechnologies.net/Documents/Airfoil.htm>